Nonperturbative comparison of clover and HISQ quarks in lattice QCD and the properties of the ϕ meson

Bipasha Chakraborty,[1,2,*] C. T. H. Davies,[1,†] G. C. Donald,[3] J. Koponen,[1,4] and G. P. Lepage[5]
(HPQCD collaboration),[‡]

[1]*SUPA, School of Physics and Astronomy, University of Glasgow, Glasgow, G12 8QQ, UK*
[2]*Jefferson Lab, 12000 Jefferson Avenue, Newport News, Virginia 23606, USA*
[3]*Institute for Theoretical Physics, University of Regensburg, 93040 Regensburg, Germany*
[4]*INFN, Sezione di Tor Vergata, Dipartimento di Fisica, Università di Roma Tor Vergata, Via della Ricerca Scientifica 1, I-00133 Roma, Italy*
[5]*Laboratory of Elementary-Particle Physics, Cornell University, Ithaca, New York 14853, USA*

(Dated: September 14, 2017)

We compare correlators for pseudoscalar and vector mesons made from valence strange quarks using the clover quark and highly improved staggered quark (HISQ) formalisms in full lattice QCD. We use fully nonperturbative methods to normalise vector and axial vector current operators made from HISQ quarks, clover quarks and from combining HISQ and clover fields. This allows us to test expectations for the renormalisation factors based on perturbative QCD, with implications for the error budget of lattice QCD calculations of the matrix elements of clover-staggered b-light weak currents, as well as further HISQ calculations of the hadronic vacuum polarisation. We also compare the approach to the (same) continuum limit in clover and HISQ formalisms for the mass and decay constant of the ϕ meson. Our final results for these parameters, using single-meson correlators and allowing an uncertainty for the neglect of quark-line disconnected diagrams are: $M_\phi = 1.023(6)$ GeV and $f_\phi = 0.238(3)$ GeV in good agreement with experiment. The results come from calculations in the HISQ formalism using gluon fields that include the effect of u, d, s and c quarks in the sea with three lattice spacing values and $m_{u/d}$ values going down to the physical point.

I. INTRODUCTION

Weak decay matrix elements calculated in lattice QCD are critical to the flavour physics programme of overdetermining the Cabibbo-Kobayashi-Maskawa matrix to find signs of new physics (see, for example, [1, 2]). For this programme it is particularly important to study heavy flavour physics and, although it is now becoming possible to study heavy quarks using relativistic formalisms [3, 4], the most extensive studies of heavy quarks in lattice QCD have been done with nonrelativistic formalisms (or at least formalisms that make use of nonrelativistic methods), such as NRQCD [5] or the Fermilab formalism [6]. In nonrelativistic formalisms a critical issue is the normalisation of the current operator that couples to the W boson, and this is one of the main sources of error in the lattice QCD result. Relativistic formalisms can be chosen to have absolutely normalised currents, for example through the existence of a partially conserved axial current (PCAC) relation [7]. The main issue with relativistic formalisms is then controlling discretisation errors [8].

The archetypal heavy meson weak decay process is annihilation of a B meson to $\tau\nu$. The hadronic parameter which controls the rate of this process is the B meson decay constant, f_B, proportional to the matrix element to create a B meson from the vacuum with the temporal axial current containing a bottom quark field and a light antiquark field. When the heavy quark field uses a nonrelativistic formalism the simplest way to match the appropriate current in lattice QCD to that in a continuum scheme is using lattice QCD perturbation theory. Such calculations of the Z factors required have been done through $\mathcal{O}(\alpha_s)$ for both NRQCD [9–11] and Fermilab [12, 13] heavy quarks with a variety of different light quark formalisms. The most recent results for B meson decay constants using NRQCD are given in [14] and using Fermilab heavy quarks in [15].

In doing these calculations for Fermilab heavy quarks and clover light quarks [12] it was noticed that the heavy-light current renormalisation differed very little at $\mathcal{O}(\alpha_s)$ from the square root of the product of Z factors for the temporal vector heavy-heavy and light-light currents, which can be determined nonperturbatively. This then gives rise to the possibility of determining, for example, $Z_{A^4{}_{hl}}$ with small uncertainty if it can be demonstrated that this result is true to all orders in perturbation theory and is not specific to only one light quark formalism (or heavy quark formalism). This question is a critical one for the reliability of the estimates of perturbative errors in determinations of f_B and f_{B_s} and other weak matrix elements using this approach. The same issues arise, for example, for the vector current with implications for the matrix elements calculated for $B \to \pi\ell\nu$ from lattice QCD [16].

Here we test this fully nonperturbatively for the case where the 'heavy-light' current is made of a clover quark ($\equiv$ Fermilab formalism at low mass) and a highly im-

*bipasha@jlab.org
†christine.davies@glasgow.ac.uk
‡URL: http://www.physics.gla.ac.uk/HPQCD

proved staggered quark (HISQ) [8] both tuned accurately to the strange quark mass, following the suggestion in [1]. We use the absolute normalisation for the HISQ-HISQ temporal axial vector current that arises from chiral symmetry in that formalism to normalise both the HISQ-clover and clover-clover temporal axial vector current. By determining the normalisation of the appropriate vector currents, also fully nonperturbatively, we can then determine the ratio used by the Fermilab collaboration and test it against the hypothesis that it should be close to 1.

From the same s quark propagators for the study above we can also make vector (ϕ) meson correlators and study the ϕ meson mass and decay constant for the cases where the ϕ is made purely of clover quarks or purely of HISQ quarks, or made of one of each. Our results cover 3 values of the lattice spacing spanning the range from 0.15 fm to 0.09 fm and so we can compare the approach to the continuum limit of the two formalisms (and test whether they have a common continuum limit) for the two calculations.

Finally we make a more extensive analysis of the ϕ meson using the HISQ formalism covering a more complete range of gluon field ensembles that includes multiple values of the u/d quark mass in the sea going down to the physical value, and allowing physical results to be derived. Our calculation uses single-meson correlators only and neglects quark-line disconnected diagrams (which we expect to have negligible impact). Our results tend to confirm that the impact of coupling the ϕ to its $K\overline{K}$ decay mode is small and increases the u/d quark mass-dependence of the ϕ properties determined in lattice QCD. We are able to obtain the ϕ mass and decay constant to an accuracy of a few MeV and in agreement with experiment. Understanding the properties of the ϕ from lattice QCD is important because it provides a good vector final state for alternative studies of semileptonic weak decay rates compared to the usual pseudoscalar final states. For example, V_{cs} can be determined from $D_s \to \phi\ell\nu$ given lattice QCD results and experimental rates [17–19]. $B_s \to \phi\ell^+\ell^-$ is potentially an important rare decay mode for searches for new physics [20].

The paper is laid out as follows: Section II describes the background to our calculation; the perturbative studies of the renormalisation factors that have been done for current operators using different actions and combinations of actions, and the general picture that emerges that needs to be tested nonperturbatively. Section III describes our lattice calculation to do these tests and gives our results for the nonperturbative determination of Z factors for the HISQ-clover and clover-clover case, showing how the nonperturbative determination backs up the picture seen perturbatively. We also compare discretisation effects in the clover and HISQ formalisms through the properties of the ϕ meson using the Z factors we have obtained to normalise the decay constant. Section IV gives our results for the mass and decay constant of the ϕ in the HISQ formalism only, covering u/d quark masses down to the physical value and allowing a chiral/continuum extrapolation to the physical point. Section V gives our conclusions. Appendix A considers the renormalisation factors for currents with NRQCD heavy quarks and Appendix B uses our results for the renormalisation factors for local vector currents for HISQ quarks to extrapolate to values on finer lattices.

II. BACKGROUND

To provide accurate physical results for hadronic matrix elements, lattice QCD current operators must be renormalised to match to those in continuum QCD. For some currents and quark formalisms absolute normalisation is possible; for example for the temporal axial current in formalisms with sufficient chiral symmetry. In other cases a renormalisation Z factor must be determined as accurately as possible. Since the Z factor, beyond tree-level, allows for the difference between gluon radiation in the continuum and that in the presence of the lattice momentum cut-off, it is an ultra-violet quantity and can be determined in QCD perturbation theory. Lattice QCD perturbation theory is relatively complicated and such calculations have generally been restricted to the determination of effects at $\mathcal{O}(\alpha_s)$ only. Z is then determined by equating the one-loop scattering amplitude between on-shell quark states in continuum QCD and on the lattice.

Early calculations in which a heavy quark in the Fermilab formalism [6] was combined with a clover light quark found that the heavy-light current renormalisation [12] differed very little at $\mathcal{O}(\alpha_s)$ from the square root of the product of Z factors for the temporal vector heavy-heavy and light-light currents. This was found also to be true for Fermilab heavy quarks and asqtad light quarks [13]. Specifically, the Fermilab Lattice collaboration writes for the temporal axial vector current:

$$Z_{A^4{}_{hl}} = \rho\sqrt{Z_{V^4{}_{hh}} Z_{V^4{}_{ll}}} \tag{1}$$

where

$$\rho = 1 + \rho^{(1)}\alpha_s + \rho^{(2)}\alpha_s^2 + \ldots \tag{2}$$

and $\rho^{(1)}$ is found to be very small (typically $< 4\pi \times 0.01$) if the heavy quark mass is not too large. Note then that this is a relationship valid for 'light' heavy quarks and not in the infinite quark mass (static) limit. In practice the region of small values of $\rho^{(1)}$ extends for heavy quark masses, m_h, in the Fermilab formalism up to the b quark mass at least for fine lattices, with $a < 0.1$ fm. For small values of m_h the Fermilab formalism becomes identical to the standard tadpole-improved clover formalism.

$Z_{V^4{}_{hh}}$ and $Z_{V^4{}_{ll}}$ are the renormalisation factors for local temporal vector currents made respectively of Fermilab formalism quarks and light quarks in whatever formalism is being used for the heavy-light current. These vector current Z factors can be determined fully nonperturbatively in lattice QCD by demanding normalisation

of the vector form factor between two identical mesons at rest.

Eq. (1) then gives rise to the possibility that $Z_{A^4{}_{hl}}$ can be determined with small errors if it can be shown that ρ is indeed close to 1 to all orders in perturbation theory. The argument that this should be true is based on the idea that a large part of the perturbative Z comes from the self-energy of the individual quark legs and this part will cancel in ρ [12]. This cancellation will include tree-level mass dependence and tadpole effects. However, this only guarantees that $\rho^{(2)}$ and higher coefficients should be 'of reasonable size', not that they should be as small as $\rho^{(1)}$ is found to be. The question of what uncertainty it is reasonable to take for the missing α_s^2 and higher order pieces is then a critical one for the reliability of the estimates of perturbative errors in determinations of f_B and f_{B_s} and other weak matrix elements using this approach.

In testing this relationship nonperturbatively we note that to be robust it must be fairly general and work for a variety of formalisms, for example any light quark formalism combined with a Fermilab formalism heavy quark. Since in fact it is a relationship that works best for light quarks in the Fermilab formalism, we can substitute standard clover quarks for Fermilab quarks since the Fermilab formalism becomes the clover formalism in the light quark mass limit. This avoids then any need to handle Λ/m_h (where m_h is the heavy quark mass) corrections to the 'heavy-light' currents.

We then test eq. (1) for the case where the current on the lefthandside contains two light quarks that use different formalisms. One formalism is clover, representing the Fermilab formalism. For the other formalism we could use the asqtad staggered formalism to test directly the results from [13]. However it makes more sense to use the current state-of-the-art staggered formalism, HISQ [8], since we will also use the state-of-the-art MILC collaboration gluon field configurations that include u, d, s and c quarks in the sea using the HISQ formalism. We will tune the masses of the valence light quarks to that of the strange quark because this can be done very accurately [21, 22] using the pseudoscalar 'strange-onium' meson, the η_s and will give higher statistical accuracy for this test than using lighter quarks.

Because the HISQ formalism has a remnant chiral symmetry it has an absolutely normalised temporal axial current. By comparing the matrix element between the vacuum and the η_s of temporal axial currents made of clover quarks or mixed currents with one clover and one HISQ quark to that made of HISQ quarks we can determine the Z factor for the clover-clover current and the HISQ-clover current. We can also readily determine the Z factors for the local temporal vector current made of HISQ quarks or of clover quarks, or the mixed HISQ-clover current, by setting the vector form factor to 1 between two η_s mesons made of appropriate quark formalisms at rest.

We then have all the Z factors necessary to test the relationship equivalent to eq. (1):

$$Z_{J_{\mathrm{H-cl}}} = \rho_J \sqrt{Z_{V^4{}_{\mathrm{cl-cl}}} Z_{V^4{}_{\mathrm{H-H}}}}, \tag{3}$$

where H stands for HISQ and cl for clover, for the cases where the current J is the temporal axial current or the temporal vector current. In both cases we can determine how close to 1 ρ_J is and therefore how small the perturbative coefficients that make up ρ_J must be.

As a side-product of these calculations we can test a number of other relationships between Z factors, including that between the temporal axial vector and temporal vector currents in all three combinations of formalisms, H-H, H-cl and cl-cl. Note that the Z factor being determined on the lefthandside of eq. (1) is a flavour-nonsinglet current. Our equivalent expression, implied by eq. (3), then also corresponds to a flavour-nonsinglet current even though both quarks are s quarks. This means that we do not need to consider any quark-line disconnected contributions to the correlation functions that we are using for this analysis. The Z_V factors on the righthandside of eq. (1) correspond to vector currents for quarks of the same flavour; in this case quark-line disconnected contributions are negligible [23] and can be ignored.

The next section describes the lattice calculation and gives results for these Z factors.

Set	β	w_0/a	am_l^{sea}	am_s^{sea}	am_c^{sea}	L_s/a	L_t/a
1	5.80	1.1119(10)	0.013	0.065	0.838	16	48
2	5.80	1.1367(5)	0.00235	0.0647	0.831	16	48
3	6.00	1.3826(11)	0.0102	0.0509	0.635	24	64
4	6.00	1.4029(9)	0.00507	0.0507	0.628	24	64
5	6.00	1.4029(9)	0.00507	0.0507	0.628	32	64
6	6.00	1.4029(9)	0.00507	0.0507	0.628	40	64
7	6.00	1.4149(6)	0.00184	0.0507	0.628	48	64
8	6.30	1.9006(20)	0.0074	0.0370	0.440	32	96
9	6.30	1.9518(7)	0.0012	0.0363	0.432	64	96

TABLE I: Sets of MILC configurations used here with their (HISQ) sea quark masses, m_l ($m_u = m_d = m_l$), m_s and m_c in lattice units. $\beta = 10/g^2$ is the QCD gauge coupling and w_0/a [22, 24] gives the lattice spacing, a, in terms of the Wilson flow parameter, w_0 [25]. The lattice spacing is approximately 0.15 fm for sets 1 and 2; 0.12 fm for sets 3-7 and 0.09 fm for sets 8 and 9. The lattice size is $L_s^3 \times L_t$. Ensemble sizes are 500 to 1000 configurations each.

III. Z FACTORS

A. Lattice configurations and simulation parameters

We use gluon field ensembles generated by the MILC collaboration [26] at widely differing values of the lattice spacings: 0.15 fm, 0.12 fm and 0.09 fm. The relative lattice spacings were fixed using a determination of

Set	$am_s^{H,val}$	$\kappa_s{}^{cl,val}$	u_0	n_{cfg}	n_t	3pt T
1	0.0705	0.14082	0.85535	1021	12	9, 12, 15, 18
3	0.0541	0.13990	0.86372	527	16	12, 15, 18, 21
8	0.0376	0.13862	0.87417	504	16	16, 19, 22, 25

TABLE II: List of parameters used for the valence quarks. Column 2 gives the HISQ bare mass. Columns 3 and 4 give the clover κ value and the tadpole factor u_0 used to tadpole-improve the action. Column 5 gives the number of configurations used for most of the calculations and column 6 the number of time sources on each configuration. Because our HISQ valence quarks are much faster to calculate we have determined η_s H-H correlators on double the number of configurations for sets 3 and 8. We only determined the 3-point correlators for the H-cl current on half of the configurations on set 8, however. The final column gives the T values used in the determination of 3-point correlation functions.

w_0/a [22] [1] where w_0 is the Wilson flow parameter [25]. The absolute value of w_0 was determined from f_π [22] to be 0.1715(9) fm. The gluon field ensembles include the effect of u, d, s and c quarks in the sea (with degenerate u and d quarks) using the HISQ formalism and also use a gluon action improved fully through $\mathcal{O}(\alpha_s a^2)$ [27]. We therefore expect the gluon fields to have very small 'intrinsic' discretisation errors which is useful for studying the discretisation errors of meson correlation functions made on these configurations using different quark formalisms.

For our determination of clover Z factors we have chosen to use the ensembles 1, 3 and 8 that have a sea light quark mass in units of the sea strange mass $m_l/m_s = 0.2$. This is for reasons of numerical speed since these lattices have relatively modest size of 3.5 fm. Since we are calculating meson correlation functions made purely of strange quarks, we expect sea quark mass effects to be small so the fact that $m_l^{\rm sea}$ is not physical is not an issue. Finite volume effects were shown to be negligible for the η_s for lattices of size 3.5 fm in [28] (see also Section IV). In any case we would expect such effects to be the same for the HISQ and clover valence quarks and hence any effects should cancel in the ratios we use to determine Z factors.

On gluon field ensembles 1, 3 and 8 we calculate valence HISQ and clover quark propagators using the standard HISQ action [8] (as used for the sea quarks) and the standard tadpole-improved space-and-time-symmetric clover action used for light quarks [29]. In the clover action the gluon fields U_μ are divided by a tadpole parameter [30], u_0, for which we use the fourth root of the plaquette. The parameter values are listed in Table II.

For the source for each propagator we divide the spatial slice of the lattice at a given time value into 2^3 cubes and use a Gaussian random number for each color at the spatial points corresponding to the corners of each cube. We use many time sources on each configuration to improve statistics (see Table II) and they are evenly spaced through the lattice. The starting time source for each configuration is chosen randomly to reduce autocorrrelations, which are small for η_s correlators [31].

We combine the HISQ propagator with its complex conjugate into a pseudoscalar meson correlator (two-point function) that corresponds to the 'Goldstone taste' in the parlance of staggered quarks. In spin-taste notation this is $\gamma_5 \otimes \gamma_5$ and the correlator simply corresponds to the modulus squared of the propagator, summed over a spatial slice of the lattice to project onto zero spatial momentum. We will denote the ground-state particle of this correlator $\eta_s^{\rm H-H}$. To obtain the ground-state parameters we fit the correlator to the standard multi-exponential form as a function of time separation t between the source and sink:

$$\begin{aligned} C_{2pt} &= \sum_{k=0}^{n_{\rm exp}-1} a_k^2 f(E_k,t); \\ f(E_k,t) &= e^{-E_k t} + e^{-E_k(L_t-t)}. \end{aligned} \quad (4)$$

There are no staggered quark 'oscillating' terms in the η_s correlator because it is of Goldstone taste and made of equal mass quarks. Our fits use Bayesian methods [32] that allow us to include multiple exponentials and consequently allow for systematic errors in our ground-state parameters from contamination from excited states. We use a prior width on all of the amplitudes of 0.5 (larger than any of our ground-state amplitudes) and on the ground-state energy of 0.05 (much larger than any of our fit uncertainties on this parameter). On the energy differences between consecutive states we take a prior of 0.8(0.4) GeV (converted back to lattice units in the fit). We have checked that the ground-state parameters from our fit are very insensitive to the priors. We drop the very small t values from the fit, taking $t_{\rm min}$ of 3 or 4. Fit results and uncertainties are stable from 3 or 4 exponentials upwards with χ^2/dof varying from 0.5 to 0.9. We take our final values from the 6 exponential fit. Neither the number of exponentials in the fit, nor the $t_{\rm min}$ value have any significant effect on the result for ground-state parameters. We illustrate this in Figure 1, giving the ground-state energy from the fit as a function of the number of exponentials included for both $t_{\rm min}$ of 3 (the value we used) and $t_{\rm min} = 10$. For $t_{\rm min}$ of 3 fits with a small number of exponentials (1 and 2) give a poor fit because higher states contribute to the correlator at small t values. However, once the fit does have a good χ^2 it remains stable as further states are added to the fit. For $t_{\rm min}$ of 10 a good fit can be obtained with fewer states included and it agrees with the result using $t_{\rm min} = 3$. We prefer to take the smaller $t_{\rm min}$ value for uniformity of fits across all the 2- and 3-point functions we study here.

Here we are concerned with the properties of the ground-state, which are given by $k = 0$. These are the

[1] Note that the value on set 8 has changed from that given in [22]; we are grateful to C. McNeile for providing this updated value.

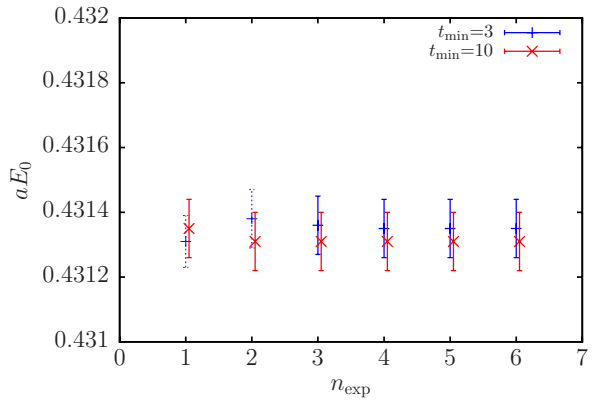

FIG. 1: Results for the ground-state energy, E_0 in lattice units, for the H-H η_s on coarse set 3 as a function of the number of exponentials used in the fit (eq. (4)). We show results for a $t_{\rm min}$ value of 3 and 10; the results are shown with dashed lines for fits where the $\chi^2/[\rm dof] > 1$.

mass of the $\eta_s^{\rm H-H}$ which is given in lattice units by E_0 and its decay constant which is determined from the ground-state amplitude, a_0, as described in section III B.

Earlier results [22] using a variety of both u/d and s HISQ valence masses on the more complete set of ensembles from Table I allowed us to determine the value of the η_s mass in the continuum and chiral limits of full lattice QCD. Although the η_s meson is not a physical particle (because we do not allow it to mix with other flavourless pseudoscalars) it is nevertheless useful in lattice QCD for tuning the s quark mass [21]. In [22] we obtained a physical value for the η_s mass of 688.5(2.2) MeV. Here we then tune the bare quark mass in our HISQ action to obtain this value for the $\eta_s^{\rm H-H}$ mass (combining our results for E_0 from eq. (4) with the values of the lattice spacing from Table I) on each ensemble. The bare valence quark masses obtained are given in Table II. Note that these values are not the same as those used in [22] because, with the benefit of those results, we have improved the tuning (see also [24]). The η_s mass values in lattice units (E_0 from our fits) are given in Table III. The precision of the values shows how well this tuning can be done.

We also combine clover quark propagators with their complex conjugates to make η_s correlators using either the temporal axial current, $\overline{\psi}\gamma_4\gamma_5\psi$, or the pseudoscalar current, $\overline{\psi}\gamma_5\psi$, at both source and sink. We then fit these correlators simultaneously to the same fit form, eq. (4), given earlier for the H-H case and using the same priors. We require both correlators to have the same energies but different amplitudes, a_{k,A^4} and $a_{k,P}$. Again the ground-state parameters are given by $k = 0$ and are the ones we use here. The ground-state $\eta_s^{\rm cl-cl}$ mass is given by combining values for E_0 with the inverse lattice spacing obtained from Table I. The mass parameter in the clover action is denoted by κ with the bare quark mass being related to $1/(2\kappa)$ by an additive constant [29]. We tune κ to give the same η_s mass as that discussed for the H-H case above. Table II gives the tuned κ values we obtain and Table III gives the η_s masses in lattice units (E_0 from our fits). Again we are able to perform this tuning very precisely.

The third option is to combine a clover and HISQ propagator to make a mixed-action correlator. To do this the HISQ propagators, which have no spin component, must be converted back to naive quark propagators with a spin component by 'undoing' the staggering transformation used to obtain the staggered quark action [8, 33]. Because we have used a 'corner wall' source for our propagators, with one point per 2^3 block, the matrices implementing the staggered transformation at the source are all the unit matrix, which simplifies the combination. Once converted to a naive form with 4 spin components the HISQ propagators can be straightforwardly combined with clover propagators as in the clover-clover case above and using a temporal axial current operator at source and sink, or a pseudoscalar operator. To fit these correlators (simultaneously) we must include oscillating terms that arise from the staggered quark formalism. The fit form is then

$$C_{2pt}(t) = \sum_{k=0}^{n_{exp}} a_k^2 f(E_k, t) - (-1)^{t/a} \sum_{ko=0}^{n_{exp}} a_{ko}^2 f(E_{ko}, t) \quad (5)$$

with normal (non-oscillating) amplitude parameters a_k, and amplitudes for oscillating terms given by a_{ko}. Again we use priors for the normal terms that are the same as those given above for both the H-H and cl-cl cases. For the oscillating terms we use the same amplitude and energy difference priors as for the normal terms and we take the difference between the energy for the ground-state in the oscillating channel and that in the normal channel to be 0.6(4) GeV. We again take the fit results from the 6 exponential fit, given stability of the results from the 3 or 4 exponential fit upwards. Since the mass parameters have now all been tuned, the mass we obtain for the ground-state particle in this H-cl channel gives us information about discretisation effects. These masses are given in Table III and we can see that they become increasingly close to the masses for the H-H and cl-cl channels as the lattice spacing becomes smaller moving from set 1 to set 8. This will be discussed further in Section III F.

B. Z factors for A^4

The decay constant of the η_s meson can be defined as the matrix element between the meson and the vacuum of the temporal axial current. When the meson is at rest this is given by

$$\langle 0|A^4|\eta_s\rangle = M_{\eta_s} f_{\eta_s}. \quad (6)$$

Set	Action comb'n	aM_{η_s}	af_{η_s}	af_{η_s}/Z_{A^4}	Z_{A^4}
1	H-H	0.54024(15)	0.14259(8)	-	
	cl-cl	0.53966(30)		0.19682(26)	0.7245(10)
	H-cl	0.57330(24)		0.16303(24)	0.8746(13)
3	H-H	0.43135(9)	0.11399(4)	-	
	cl-cl	0.43141(20)		0.15242(18)	0.7478(9)
	H-cl	0.44698(17)		0.12946(16)	0.8804(11)
8	H-H	0.31389(7)	0.08287(4)	-	
	cl-cl	0.31328(12)		0.10664(16)	0.7771(12)
	H-cl	0.31821(11)		0.09338(13)	0.8874(12)

TABLE III: Results from the fits to η_s meson correlators made from HISQ-HISQ, clover-clover and HISQ-clover s quark propagators. Column 3 gives the ground-state mass in lattice units. The H-H and cl-cl results are very close as a consequence of tuning the bare mass parameters in the HISQ and clover actions. Column 4 gives the η_s decay constant in lattice units for the H-H case where it is absolutely normalised. Column 5 gives the unnormalised η_s decay constant for the cl-cl and H-cl cases. Column 6 gives the Z factors for the cl-cl and H-cl cases from setting the decay constant equal to that in the H-H case.

For the HISQ action, remnant chiral symmetry gives a partially conserved axial current (PCAC) relation connecting the temporal axial and pseudoscalar currents for the Goldstone taste pseudoscalar that we use here. Thus we can determine an absolutely normalised decay constant from the relation

$$f_{\eta_s} = 2m_s a_0 \sqrt{\frac{2}{E_0^3}} \tag{7}$$

where E_0 and a_0 are the ground-state energy and amplitude respectively from the fit given in eq. (4). Results for the decay constant in lattice units are given in Table III. These agree with those from [22] at the physical s quark mass (see Figure 3 in that reference).

For the clover action we do not have a PCAC relation and so the temporal axial current must be renormalised. We do this by equating the decay constant obtained from the ground-state amplitude in the cl-cl case to that obtained in the H-H case where we have an absolute normalisation. In the cl-cl case we can convert the ground-state amplitude from our fits obtained from meson correlation functions using the temporal axial current to an un-normalised decay constant value in lattice units using

$$af_{\eta_s}/Z_{A^4} = a_{0,A^4}\sqrt{\frac{2}{E_0}}. \tag{8}$$

The results of this determination are given for each ensemble in Table III. The renormalisation factor Z_{A^4} is then obtained by setting af_{η_s} in the cl-cl case equal to that obtained in the H-H case.

An alternative method, but one that we do not use, would be to set the cl-cl decay constant equal to the physical value of 181.14(55) MeV obtained in [22]. Because the discretisation effects seen in the H-H values of f_{η_s} are so small this would make little difference - at most 0.5% on set 1.

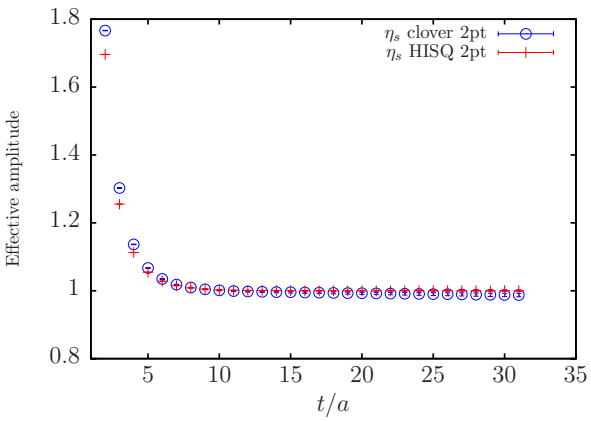

FIG. 2: The effective amplitude defined as the correlator divided by the fit result for the ground-state exponential for H-H Goldstone and cl-cl pseudoscalar η_s correlators on coarse set 3. The number of configurations used for the H-H correlators is double that of the cl-cl correlators.

Exactly the same arguments and procedure apply to determining af_{η_s}/Z_{A^4} and Z_{A^4} in the H-cl case. In this case, because the η_s mass is not exactly the same as the tuned value there is a difference between matching decay constants and matching matrix elements ($f_{\eta_s}M_{\eta_s}$). Because the difference in mass is a discretisation effect we have chosen to match decay constants. The differences between doing this and matching the matrix element $f_{\eta_s}M_{\eta_s}$ are as large as 6% on set 1, but fall to 1% on fine set 8, and act in the direction of making Z_{A^4} smaller than that quoted. We can use this variation to assess the size of nonperturbative effects appearing in our nonperturbative determination of the Z factors. A 6% effect on the coarsest lattices is not a surprising result; $(a\Lambda)^2$ with Λ around a few hundred MeV would give something similar.

The values of Z_{A^4} for the cl-cl and H-cl current are then given in column 5 of Table III.

Figure 2 illustrates directly how similar the H-H and cl-cl correlators in terms of their t-dependence. The figure shows the result in each case of dividing the correlator (with the pseudoscalar current at source and sink) by the fit function $a_0^2 f(E_0, t)$ corresponding to the ground state. The central value of both effective amplitudes is then 1 at large times. The statistical uncertainties in the H-H case are about 2.5 times smaller than the cl-cl case when double the number of configurations was used. The results for the two amplitudes agree well away from the central plateau region, showing that the contributions of excited states to the correlators are also well matched. Discretisation errors give differences at small times.

Another interesting feature of Figure 2 is that the statistical error in the correlator increases with time, albeit slowly. In the simplest picture of how noise arises in meson correlators this would not happen because the signal

to noise ratio should be a constant for pseudoscalar meson correlators made of quarks with equal mass. The variance of the meson correlator is a correlator made of two quarks and two antiquarks. When the quark masses are the same the ground-state energy of this combination is twice that of the meson that controls the signal, in the absence of interactions between the two mesons and ignoring a 'crossed' diagram that would need to be calculated to determine fully the two-meson correlator. It is these latter two effects that complicate the simple picture and cause the mass controlling the noise to fall below that controlling the signal so that an exponentially growing (albeit slowly) noise-to-signal ratio results. See [34–36] for earlier discussion and analysis of correlator noise.

C. Z factors for V^4

The normalisation of temporal vector currents in lattice QCD is readily obtained by demanding that the vector form factor be 1 between two identical states at rest. Here we can implement this for η_s states so that

$$Z_{V^4}\langle\eta_s|V^4|\eta_s\rangle = 2M_{\eta_s}. \tag{9}$$

The matrix element of the vector current is calculated from a 3-point function as illustrated in Figure 3. Propagator 2 is generated from propagator 1 as a source and then joined at the temporal vector vertex to propagator 3. Appropriate spin combinations are taken at the two ends to ensure that source and sink correspond to pseudoscalar mesons. Sums over spatial slices ensure that source and sink mesons are at rest. We use 4 values for the value of T at the end-point of the 3-point function. This enables us to fit both the t-dependence (for $0 \le t \le T$) and the T-dependence of the 3-point function to reduce systematic errors from excited state contamination. The values used for T are listed in Table II.

By choosing combinations of HISQ and clover propagators we can determine the renormalisation factor for H-H, cl-cl and H-cl temporal vector currents. The temporal vector currents we consider are all local operators and for the H-H case this corresponds to the spin-taste structure $\gamma_4 \otimes \gamma_4$. Because this current is not a taste-singlet we cannot use a three-point function made purely of staggered quarks but must have a non-staggered 'spectator' quark (propagator 1 in Figure 3). Here it is natural to use a clover s quark, extending our earlier method that used NRQCD quarks [37], itself based on a Fermilab Lattice/MILC method that uses clover quarks [15].

First we discuss the case of the cl-cl temporal vector current. For this case, all propagators are clover s quarks and we use the pseudoscalar operator at the source and sink to make η_s mesons. We make this choice because the pseudoscalar operator gives somewhat more precise correlators; the 2-point functions are simply the squared modulus of the propagator in that case. We then fit the three-point functions from all T values simultaneously

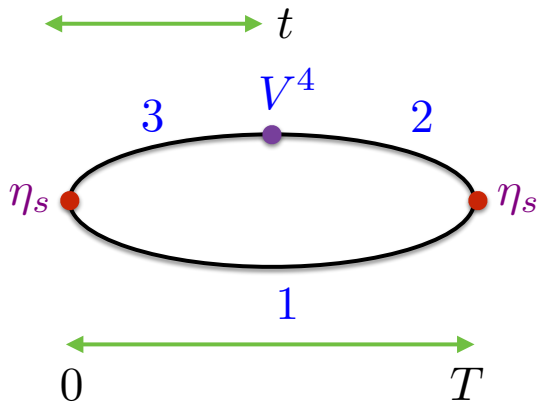

FIG. 3: A diagram to show how our three-point correlation functions are constructed. All of the quark propagators, denoted 1, 2 and 3 are for s quarks and combined at times 0 and T to make η_s mesons. A temporal vector current is inserted at t.

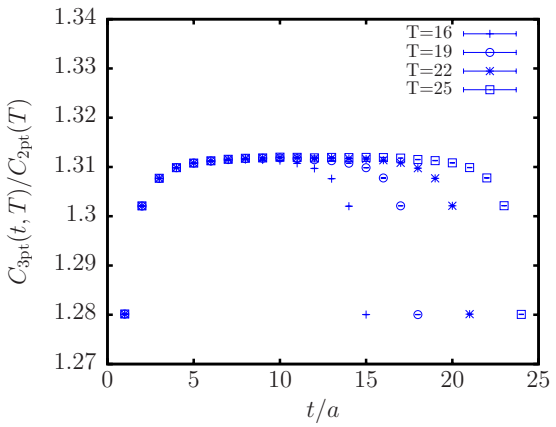

FIG. 4: The ratios of the average three-point correlator to average two-point correlator showing how the same plateau value is reached for four different values of T: 16,19,22 and 25 using the clover action on fine set 8. Statistical errors are shown on the points.

with two-point cl-cl (using γ_5 at source and sink) η_s correlators. The fit form for the three-point function is given by:

$$C_{3pt} = \sum_{i,j} a_i V_{ij} a_j f(E_i, t) f(E_j, T-t) \tag{10}$$

where a_i and a_j are amplitudes from the two-point functions (eq. (4)). We use a prior width on the V_{ij} of 0.0(3.0) (along with priors on all other parameters as for the earlier two-point correlator fits). Using a relativistic normalisation of states the matrix element of the lattice temporal vector current between ground-state η_s mesons at rest is given by $2E_0V_{00}$ and therefore

$$Z_{V^4} = \frac{1}{V_{00}}. \tag{11}$$

Our results for each of sets 1, 3 and 8 are listed in Table IV. Notice that the numbers are a lot more precise than those for Z_{A^4}. Figure 4 plots the ratio of the three-point correlator for each value of T to that of the two-point correlator at T, as a function of t to illustrate the quality of our results. From eq. (10) this ratio will be $1/V_{00}$ for all values of t, up to contamination from excited states. It is clear from Figure 4 that this contamination is under good control, with all three-point functions showing a good plateau at the same value. Note, that we do not use this ratio in our fits, but instead perform a full multi-exponential fit to our correlators as given in eqs. (10) and (4).

For the H-H local temporal vector current we have a H-cl η_s correlator at source and sink (made with a γ_5 operator). This means that there are additional oscillating terms in the fit form for the three-point function in a simultaneous fit with the appropriate two-point correlators. The fit function is then

$$\begin{aligned} C_{3pt} &= \sum_{i,j} a_i V_{ij} b_j f(E_i,t) f(E_j, T-t) \\ &\quad -(-1)^{t/a} \sum_{i,jo} a_i V_{ijo} b_{jo} f(E_i,t) f(E_{jo}, T-t). \\ &\quad -(-1)^{t/a} \sum_{io,j} a_{io} V_{ioj} b_j f(E_{io},t) f(E_j, T-t). \\ &\quad + \sum_{io,jo} a_{io} V_{iojo} b_{jo} f(E_{io},t) f(E_{jo}, T-t). \end{aligned} \tag{12}$$

Again a_i, b_j, a_{io} and b_{jo} are amplitudes that appear in the two-point correlator fit (eq. (5)). We take a prior width on V_{ij} of 0.0(3.0) and on the other V of 0.0(1.0). Again the renormalisation factor for the local temporal vector current is given by eq. (11) and our values are given in Table IV. These results improve on the values used by us [28, 38] in the calculation of the hadronic vacuum polarisation contribution to the anomalous magnetic moment of the muon.

Lastly the H-cl temporal vector current is obtained from three-point functions in which propagator 3 is a HISQ quark and 1 and 2 are clover quarks, using the γ_5 operator to construct mesons. Again we fit the three-point correlators simultaneously with the appropriate two-point correlators. Here we need both H-cl and cl-cl two-point correlators. Our three-point function fit form has oscillatary terms on the side corresponding to the H-cl two-point function but none on the side corresponding to the cl-cl twopoint function, so the fit form is the first two lines of eq. (12). We use the same priors as above and again the renormalisation factor for the local temporal vector current is given by eq. (11). Note that in using this equation we are ignoring small discretisation effects between the H-cl η_s mass and the cl-cl η_s mass evident in Table III. Including this effect changes the Z_V value by less than 0.05% even on the very coarse lattices. Our results are given in Table IV.

We see in Table IV that the values for Z_{V^4} are very similar to those for Z_{A^4} in the H-cl and cl-cl cases, despite being rather far from 1. This does add weight to the idea that there is a component of the Z factor that comes from the 'clover wavefunction renormalisation' and could be cancelled in ratios.

Set	Action comb'n	Z_{A^4}	Z_{V^4}	ρ_{A^4}	ρ_{V^4}
1	H-H	-	0.9881(10)	-	-
	cl-cl	0.7245(11)	0.7262(2)	-	-
	H-cl	0.8746(13)	0.8660(7)	1.0325(16)	1.0223(9)
3	H-H	-	0.9922(4)	-	-
	cl-cl	0.7478(9)	0.7397(3)	-	-
	H-cl	0.8804(11)	0.8739(7)	1.0277(12)	1.0201(8)
8	H-H	-	0.9940(5)	-	-
	cl-cl	0.7771(12)	0.7620(3)	-	-
	H-cl	0.8874(12)	0.8839(8)	1.0196(14)	1.0156(10)

TABLE IV: Column 4 gives results for the renormalisation factor for the local temporal vector current for each of the different action combinations and each ensemble listed in columns 1 and 2. Results for Z_{V_4} in the H-H case are more precise than those given in [28] becaue those were taken from preliminary fits. Column 3 repeats results from Table III for the temporal axial vector. Columns 5 and 6 then give the ρ factors defined in Eq. 3 for the off-diagonal H-cl combination for both temporal axial vector and temporal vector currents. Errors are statistical/fitting errors combined from the different components in quadrature.

D. Results for ρ_{A^4} and ρ_{V^4}

We now have all the ingredients necessary to test the formula for the off-diagonal-in-action renormalisation factor in terms of the square root of the product of diagonal temporal vector renormalisation factors given in eq. (3) (testing eq. (1)). We can do this for both temporal axial vector and temporal vector currents using the data in Table IV, and the results for the ρ factors are also given in that table. The ρ factors are indeed close to 1 in all cases, demonstrating that the perturbative series for ρ does have small coefficients for all powers of α_s. Note that the temporal vector and temporal axial vector ρ factors are even closer to each other than they are to 1. In Figure 5 we plot our values for ρ_{A^4} and ρ_{V^4} against the square of the lattice spacing.

In Figure 5 we also compare to the $\mathcal{O}(\alpha_s)$ perturbative result for the operator made from a combination of clover and asqtad staggered quarks in the limit that both quark masses go to zero [13]. In the clover-asqtad case the $\mathcal{O}(\alpha_s)$ coefficient for ρ for both A^4 and V^4 is $+4\pi \times 3.04 \times 10^{-3} = 0.0382$ [2], the same because of the chiral symmetry of the asqtad action. In Figure 5 we combine this coefficient with a value of α_s determined in the V-scheme at scale $2/a$ which corresponds approximately to

[2] Note a typographical error in [13] has introduced a minus sign.

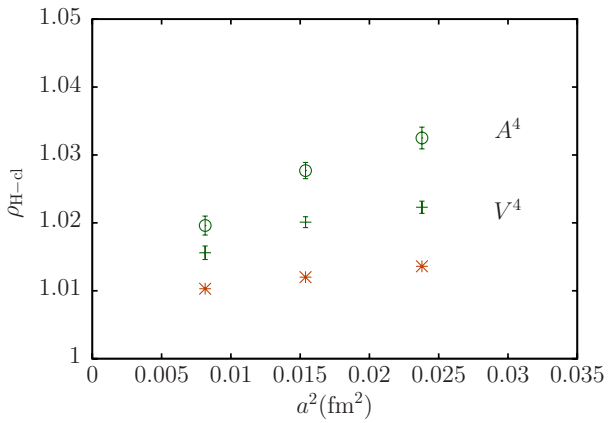

FIG. 5: Our nonperturbative results for the ρ factors defined in eq. (3) and given in Table IV for current operators made by combining HISQ and clover quarks. Green open circles gives results for the temporal axial vector current A^4 and green pluses the results for the temporal vector current V^4. Also shown are the one-loop perturbative lattice QCD results for mixed asqtad-clover currents with light clover quarks (orange bursts)

the BLM scale found for these operators in the clover-clover case [12]. The appropriate values of α_s on sets 1, 3 and 8 are: 0.356, 0.314 and 0.269. From these values it is clear that missing α_s^2 terms in the perturbative expansion could be sizeable; a coefficient of 1 would give a 10% shift to ρ.

Since we are using the HISQ action for the staggered quark and not the asqtad action, the perturbative results quoted above are not correct for our case, and are provided purely for a qualitative comparison. However we see that the nonperturbative H-cl and the one-loop perturbative asqtad-cl results have similar values and behave in a similar way with lattice spacing. The nonperturbative results are slightly further from 1 on the coarser lattices. On the finer lattices they agree to within 1%, with the perturbative result being 1% from 1 and the nonperturbative result 2%. Any comparison of nonperturbative and perturbative results must take account of possible systematic discretisation effects in the nonperturbative results. As discussed in Section III B we can estimate these from the impact of changing our definition of Z_{A^4}. This produces a sizeable 6% effect on the coarsest lattices but falling to 1% on the finest lattices. Thus on the finest lattices we can give an error band of $\pm 1\%$ around our 2% difference from 1 for the Z factor and expect the full perturbative result to lie in this band. If the one-loop perturbative results fall in this band, as the asqtad-cl results do, we can conclude that higher order terms in the perturbative expansion are constrained at this 1% level.

Assuming that the H-cl one-loop perturbative coeffients are similar to those for asqtad-cl[3], which seems likely, we can conclude that our nonperturbative results confirm the scenario in which a one-loop perturbative QCD determination of ρ_J is a very good approximation. The uncertainty from missing higher orders in the mixed action renormalisation factor can then be assumed to be small on the basis of the known (one-loop) coefficients.

The Fermilab-MILC asqtad-clover heavy-light calculations are carried out at very different values for the clover quark mass than that of the s quark that we have used here. They find, however, that the one-loop value for ρ varies relatively slowly with mass, becoming even closer to 1 as the clover mass increases to that of the charm quark [13]. Their most recent paper on B meson decay constants [15] with Fermilab heavy quarks and asqtad light quarks uses gluon field configurations with similar lattice spacing values to those used here. They take the uncertainty from missing higher order terms in the perturbative expansion of ρ as $0.1\alpha_s^2$ with α_s taken as $\alpha_V(2/a)$ on the fine lattices. This gives a 0.7% uncertainty from missing higher orders in the perturbative matching of the heavy-light current.

Although at first sight this uncertainty looks very small for an $\mathcal{O}(\alpha_s)$ calculation we can see from our results that it is in fact reasonable, provided that the H-cl one-loop calculation gives a very similar result to the asqtad-cl one-loop coefficient. This uncertainty is compatible with the difference we see between our nonperturbative results and the one-loop perturbation theory (for asqtad-cl), allowing for discretisation effects in the nonperturbative results.

In Appendix A we show how this approach to the determination of renormalisation constants also works when the heavy quark uses the NRQCD formalism. For an NRQCD-light current the division by the square root of the Z factor for the vector light-light current removes sizeable effects in the one-loop coefficients associated with the light quark formalism for clover and asqtad light quarks; no such effect is present, or correction needed, for the NRQCD quark. Defining the heavy-light Z factor using eq. (1) then reduces the one-loop coefficient in the perturbative piece of the Z factor from around 0.3 to around 0.05, with an associated reduction in perturbative uncertainty, given the evidence shown here. For NRQCD-HISQ currents the method is no longer useful since neither NRQCD nor HISQ has significant 'wavefunction renormalisation' effects and the one-loop coefficients in Z are around 0.05 without the use of eq. (1).

We can also ask: to what extent can our results for ρ, shown in Figure 5, be used to constrain unknown higher order terms in the perturbative expansion for ρ? To test this we fit a functional form to ρ that includes a power

[3] Preliminary indications, for which we thank E. Gámiz, are that this is the case

Set	Action comb'n	aM_{η_s}	af_{η_s}/Z_{A^4}	Z_{A^4}
1	H-H $(\gamma_4\gamma_5 \otimes \gamma_4\gamma_5)$	0.5605(3)	0.1409(2)	1.0120(14)
3	H-H $(\gamma_4\gamma_5 \otimes \gamma_4\gamma_5)$	0.4396(2)	0.1135(2)	1.0042(18)
8	H-H $(\gamma_4\gamma_5 \otimes \gamma_4\gamma_5)$	0.3157(1)	0.08303(8)	0.9981(11)

TABLE V: Results from the fits to η_s meson correlators made from HISQ s quarks with the local temporal axial current operator (in spin-taste notation $\gamma_4\gamma_5 \otimes \gamma_4\gamma_5$). Column 3 gives the η_s mass for this taste of meson and columns 4 and 5 the unrenormalised decay constant and derived renormalisation for this current as discussed in the text.

series in α_s allowing for discretisation effects. We use

$$\rho(a,\alpha_s) = \sum_{i=0}^{n_i} \left[c_i + d_i(\frac{a\Lambda}{\pi})^2 + f_i(\frac{a\Lambda}{\pi})^4 \right] \alpha_s^i \qquad (13)$$

with $c_0 = 1.0$, $\Lambda = 0.5$ GeV and α_s taken in the 'V' scheme at scale $2/a$. Priors on c_i, d_i and f_i are all taken as 0(1). Good fits (with χ^2/[dof] of 0.3) are readily obtained to the results for both ρ_{A^4} and ρ_{V^4} with $n_i = 5$ (although changing n_i has very little effect). The fit result for c_1 is 0.0(1), compatible with being small, as found in the calculation for the asqtad-cl case [13]. The other c_i are not constrained by the data, however. If instead we give c_1 a prior of 0.04(4) to make it close to that for the asqtad-cl case, then c_2 is weakly constrained by the fit to be around zero with an uncertainty of 0.3. These features are again compatible with the perturbative series for ρ having small coefficients. Given an α_s coefficient for the H-cl case, an improved constraint on the α_s^2 coefficient would be possible. We show how this works in Appendix B where, given an $\mathcal{O}(\alpha_s)$ coefficient, we are able to extrapolate the Z_V results for the H-H case to finer lattices fairly accurately.

E. Further tests of renormalisation factors

In staggered formalisms there are multiple versions of bilinear operators corresponding to different 'tastes'. In determing the pseudoscalar $\bar{s}s$ meson decay constant in Section III B we used the local pseudoscalar operator (in spin-taste notation $\gamma_5 \otimes \gamma_5$) because this operator is connected to the partially conserved temporal axial current through the PCAC relation. Note that we do not actually form operators with the partially conserved temporal axial current because it is point-split and so quite complicated to implement. It is also unnecessary since we can use the simple local pseudoscalar operator. On some occasions, however, it is necessary or desirable to use an explicit temporal axial current operator. The simplest one is the local operator, in spin-taste notation $\gamma_4\gamma_5 \otimes \gamma_4\gamma_5$. This couples to the 'local nongoldstone' η_s meson which has a slightly heavier mass than the goldstone meson whose mass was used to tune the s quark mass in Section III A.

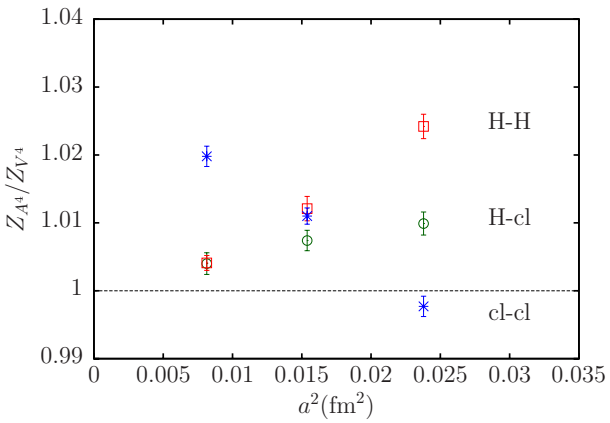

FIG. 6: The ratio of renormalisation constants for local temporal axial and local temporal vector currents made of our 3 combinations of actions: H-H (red open squares), H-cl (green open circles) and cl-cl (blue bursts). Results are plotted as a function of the square of the lattice spacing and compared to 1,shown as the grey dashed line.

Here we give results for η_s meson correlators that use this local temporal axial current operator at source and sink. The fits to these two-point correlators have staggered 'oscillations' and we use the fit form given in eq. (5). In fact we fit these correlators simultaneously with the goldstone η_s correlators, although the fits have no parameters in common. The ground-state mass, E_0, corresponds to the mass of the η_s meson of this taste and differs from the goldstone η_s mass by discretisation effects. This will be discussed further in Section III F. The ground-state amplitude, a_0, can be converted into an unrenormalised decay constant using the formula of eq. (8). As in Section III B we can define a renormalisation constant from setting this decay constant equal to that obtained from the goldstone η_s where the normalisation is absolute.

Table V gives our results on sets 1, 3 and 8 for the mass, decay constant and Z_{A^4} factor for the H-H local temporal axial current case. We see that Z_{A^4} is very close to 1 on all sets. The chiral symmetry of the HISQ action also means that Z_{A^4} for the local temporal axial vector current should equal that for the local temporal vector current [39] up to lattice artefacts and we demonstrate that this is true below.

Note that we would get slightly different values for Z_{A^4} if we matched the matrix element $(f_{\eta_s} m_{\eta_s})$ between the tastes rather than just the decay constant. This is because the meson masses differ for different tastes by an amount proportional to $\alpha_s a^2$. Since this is a pure discretisation effect, we do not include it. Doing so would give values for Z_{A^4} that are 4% lower on set 1 and 0.6% lower on set 8, and in fact then closer to Z_{V^4} on the coarser lattices.

The comparison of temporal axial vector and temporal vector Z factors can now be done for all the combinations of actions we have used - H-H, H-cl and cl-cl. The HISQ

action has sufficient chiral symmetry that the H-cl and H-H Z factors should be the same up to lattice artefacts from the nonperturbative determination that vanish as $a \to 0$, and we can test this. For H-H the appropriate Z factors are those for the local temporal vector $(\gamma_4 \otimes \gamma_4)$ from Table V and the local temporal axial vector $(\gamma_4\gamma_5 \otimes \gamma_4\gamma_5)$ from Table V. For the other cases both results come from Table IV. Figure 6 shows the ratio of Z_{A^4}/Z_{V^4} as a function of lattice spacing. We see that, although the ratio differs from 1 by 2% for H-H and 1% for H-cl on the very coarse lattices, the discrepancy between the Z factors for H-H and H-cl is falling with a^2 to agree to better than 1% on the fine lattices. Results are consistent with the Z factors being in complete agreement in the continuum limit in keeping with our expectation based on chiral symmetry.

For the cl-cl case, in the absence of chiral symmetry, we do not expect Z_{A^4} and Z_{V^4} to agree. In one-loop perturbation theory the $\mathcal{O}(\alpha_s)$ coefficient for the ratio Z_{A^4}/Z_{V^4} is +0.127 [40] for the Symanzik improved gluon fields and unimproved currents (along with $c_{sw} = 1$ to leading order in α_s) that we use here (this is somewhat smaller than the coefficent of 0.163 for the unimproved gluon field case [41, 42]). Thus we expect Z^{A^4}/Z^{V^4} to be greater than 1. This is borne out by our results in Figure 6. Our ratio is slightly below 1 on the very coarse lattices and moves above 1 going towards finer lattices, heading in the opposite direction to the other two action combinations. This is consistent with results heading towards the one-loop perturbative result, with the discrepancy on the coarser lattices being mainly a result of discretisation effects. We have seen in Section III B that discretisation effects can be $\mathcal{O}(5\%)$ on the coarsest lattices used here; they would presumably be smaller had we used an $\mathcal{O}(a)$ improved current. Using the α_s values from Section III D would give one-loop results for Z_{A_4}/Z_{V_4} of 1.045, 1.040 and 1.034 from very coarse to fine lattices to be compared with the values in Figure 6. Two-loop perturbative results for Z factors are available in the clover case [43] using an unimproved gluon action. There including two-loop terms pushes Z_{A^4} and Z_{V^4} further below 1 for $c_{sw} = 1$ but makes less difference to their ratio.

Ratios of renormalisation constants for two clover quarks are used by the Fermilab Lattice/MILC collaborations in their renormalisation of form factors involving a $b \to c$ weak transition (for example, $B \to D^*\ell\nu$ [44]). In that case the two quarks are both heavy but of different mass and eq. (1) is used with $l = c$. The perturbative analysis [45] again shows very small $\mathcal{O}(\alpha_s)$ coefficients for the ratio ρ, leading to the assumption that unknown higher order terms are also small. In this case Heavy Quark Symmetry arguments can also be used in arguments about the size of coefficients and their mass dependence. The results that we have here are for the equal mass case at small mass and so rather far from the $b \to c$ scenario. However the results for the one-loop perturbative renormalisation given above are within 1% of our nonperturbative results on the fine lattices (as can be seen in Figure 6), indicating that higher order corrections are indeed small in this case as in the H-cl case of Section III D.

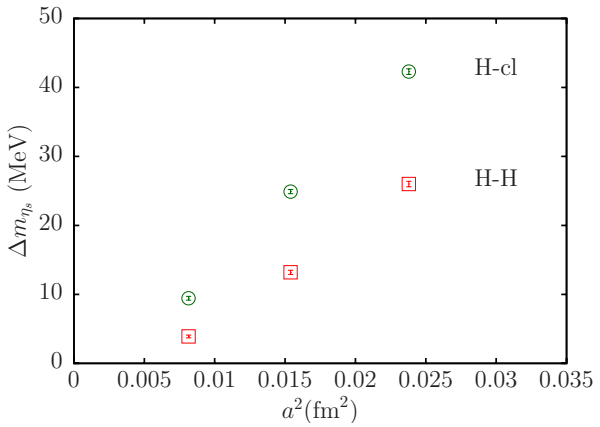

FIG. 7: The mass difference between the HISQ-HISQ local nongoldstone meson and the goldstone meson (open red squares) plotted against the square of the lattice spacing. Also shown is the mass difference between the HISQ-clover η_s mass and that of the HISQ-HISQ goldstone η_s when both HISQ and clover action are tuned to the s quark mass (green open circles). Errors include statistical errors and lattice spacing uncertainties correlated between the points.

F. Comparison of HISQ and clover discretisation effects

Systematic errors from discretisation appear differently in the HISQ and clover actions and we can test how much of an effect that is from our results. The first place in which discretisation effects show up is in differences between the masses of η_s mesons obtained with two quark propagators with the quark mass tuned to that of the s quark. Figure 7 plots two mass differences in MeV against the square of the lattice spacing. One set of points gives the mass difference between the H-cl η_s mass and that of the H-H goldstone η_s, using results from Table III. The second set gives the mass difference between two tastes of H-H η_s, the local nongoldstone and the goldstone, using results from Tables III and V. In both cases it is clear that the mass difference is purely a lattice artefact that vanishes as $a \to 0$. We expect the H-H mass difference to vanish as $\alpha_s a^2$ (since tree-level a^2 errors are absent from the action) and a^4. In fact for the finer two points a simple fit to the form $g(a\Lambda)^4 + h(a\Lambda)^6$ works well with Λ a few hundred MeV and g and h with priors 0 ± 1; to add in the coarser point requires the addition of higher orders in a^2 and/or α_s. The H-cl mass difference has $\alpha_s a$ terms from the clover action and the results are precise enough to see this. A fit to the results including $g\alpha_s(a\Lambda) + h(a\Lambda)^2 + j(\alpha_s(a\Lambda)^2)$ has a χ^2/[dof] of 0.9. The H-cl mass difference is larger and has a larger slope than

Set	Action comb'n	aM_ϕ	af_ϕ/Z_V
1	H-H	0.8183(33)	0.1994(33)
	cl-cl	0.7809(22)	0.2948(33)
	H-cl	0.8037(16)	0.2372(16)
3	H-H	0.6475(31)	0.1514(38)
	cl-cl	0.6306(26)	0.2198(44)
	H-cl	0.6413(30)	0.1789(44)
8	H-H	0.4735(13)	0.1126(12)
	cl-cl	0.4653(14)	0.1532(17)
	H-cl	0.4709(16)	0.1303(13)

TABLE VI: The results for the mass and (unnormalised) decay constants of the ϕ meson in lattice units from correlators made of s quark propagators generated using different combinations of HISQ and clover actions.

the H-H mass difference plotted in Figure 7. It should be noted that the mass difference between the Goldstone and other tastes of H-H pseudoscalar meson would be larger [8, 26] than the value plotted here for the local nongoldstone to Goldstone splitting.

Since we use the η_s decay constant to fix Z_{A^4} we cannot use that quantity to probe discretisation effects in the cl-cl or H-cl cases. That the discretisation errors are very small for the H-H case for this quantity has already been demonstrated in [22].

Two further quantities that we can study to compare discretisation effects are the mass and decay constant of the vector $\overline{s}s$ state, the ϕ. To reduce the impact of uncertainties in the lattice spacing on our results we will in fact work with the mass difference between the ϕ and the η_s. Using the experimental value of the ϕ mass, 1.01946(2) GeV [46], this difference is 0.3310(22) GeV at zero lattice spacing and physical quark masses, where the uncertainty comes from the lattice determination of the η_s mass [22].

The experimental value of the ϕ decay constant is determined from its partial width to leptons using (ignoring the spread in its mass from its full width):

$$\Gamma\left(\phi \to e^+e^-\right) = \frac{4\pi}{3}\alpha_{QED}^2 \frac{f_\phi^2}{M_\phi} e_s^2 \qquad (14)$$

Here α_{QED} at the scale of M_ϕ is $\frac{1}{137}$ and e_s is the s quark electric charge in units of e (1/3). The experimental value of the ϕ partial width $\Gamma(\phi \to e^+e^-) = 1.27(4)\,\text{keV}$ [46], giving $f_\phi = 228.5 \pm 3.6\,\text{MeV}$.

We construct vector meson correlators from s quark propagators in the same way as that described for η_s mesons, combining either two HISQ propagators, two clover propagators or a HISQ propagator and a clover propagator. The propagators are combined using the spatial version of the temporal vector current which was normalised in Section III C. We average over all three spatial directions for the current. The vector meson correlators (two-point functions) are fit as a function of time separation between source and sink using the methods and fit functions outlined in Section III A. We use the same priors as before; the only difference is that now the

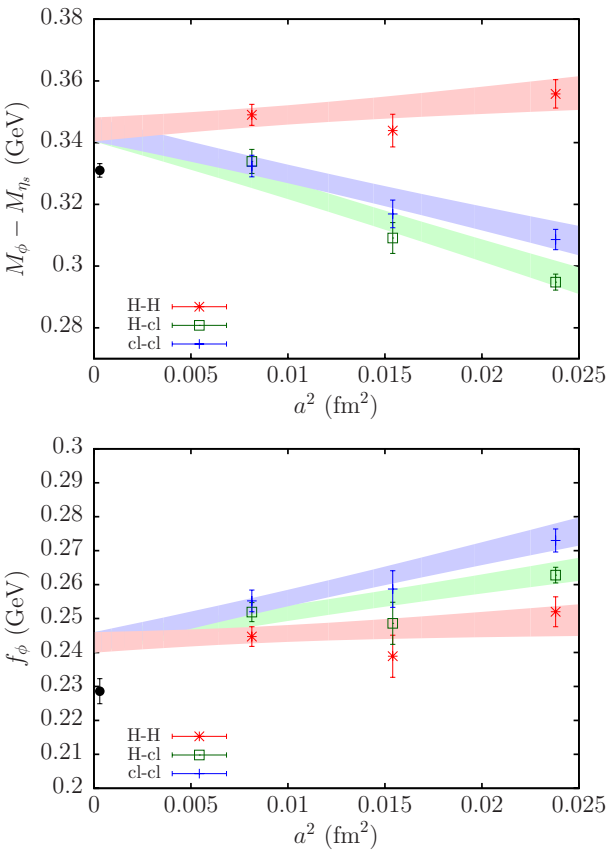

FIG. 8: Top: $m_\phi - m_{\eta_s}$ calculated with different quark formalisms and extrapolated to $a = 0$. Red bursts give results for mesons made with two HISQ quarks, blue pluses those made with two clover quarks and green open squares those made with one HISQ and one clover quark. The associated coloured bands give a simple continuum extrapolation fit with a common continuum limit, as described in the text. The black filled circle gives the value corresponding to the difference of the experimental ϕ meson mass the mass of the η_s determined from lattice QCD [22]. It is offset slightly from $a = 0$ for visibility. Bottom: f_ϕ calculated for ϕ mesons made using quarks with different formalisms and extrapolated to $a = 0$. Symbols and coloured bands are as for the top plot. The black filled circle is the value inferred from the experimental leptonic width of the ϕ (see text).

H-H correlators have an oscillating component and so we use the fit form of eq. (5) rather than eq. (4). Table VI gives results in lattice units for the ϕ mass and for its unnormalised decay constant, af_ϕ/Z_V, obtained from the ground-state amplitudes returned by the fit according to the vector analogue of eq. (8)

$$af_\phi/Z_V = a_{0,V}\sqrt{\frac{2}{E_0}}. \qquad (15)$$

To normalise the decay constant we then multiply by the renormalisation factor obtained for the temporal vector and given in Table IV, and by the inverse lattice spacing to convert to GeV units.

Results are plotted as a function of the square of the lattice spacing for each set of action combinations in Figure 8. In order to test whether all the different combinations give the same continuum limit result, as they should, we have performed a simple joint extrapolation in which we allow results for each action combination to have a different coefficient for an a^2 discretisation effect. We also include a common term allowing for the very slight mistuning of the η_s mass between lattice spacings and the mistuning of the sea masses from the nominal $m_l/m_s = 0.2$ value on different ensembles. These latter effects are very small. Such a fit is readily achieved with a good χ^2/dof below 0.9. The cl-cl and H-cl combinations in principle have $\mathcal{O}(a)$ discretisation errors coming from the clover quarks, but we are not in a position to test that with our data and allowing for this possibility would make a joint continuum limit even easier to achieve.

It is clearly visible in Figure 8 that the cl-cl and H-cl combinations have larger discretisation effects than the H-H combination, when using w_0/a to fix the lattice spacing. This is expected because the HISQ action has no tree-level a^2 errors [8] so a^2 effects are suppressed by at least one power of α_s. The clover action, even ignoring the possibility of $\mathcal{O}(a)$ errors, has $\mathcal{O}(a^2)$ errors at tree-level. We find discretisation effects for H-cl are about 4 times larger than for H-H in both the mass and decay constant. For cl-cl discretisation effects are 3 times larger in the mass and 5 times larger in the decay constant, than for H-H.

What is also seen in Figure 8 is that the continuum limit of the results is not in very good agreement with the physical value shown as a filled black circle. This is because here we are working at unphysical u/d sea quark masses. Better agreement will be seen in the next section where we map out the ϕ properties down to physical u/d quark masses, but only in the H-H case.

A further point of comparison between HISQ and clover quarks is that of statistical errors. These can be judged to some extent by looking at the fitted results for masses and amplitudes in the tables. We can also look directly at the variance of the correlators calculated on a given number of gluon field configurations. As already remarked in the context of Figure 2 the H-H correlators that use the local pseudoscalar operator at source and sink have somewhat smaller statistical uncertainties than clover ones, even allowing for the different number of gluon field configurations used. For two-point correlation functions that use the temporal axial current, or that use the vector current (see Table VI), statistical errors are very similar between the different action combinations. For the determination of Z_{V^4} using 3-point functions statistical errors are also similar between H-H and cl-cl on the finer sets 3 and 8 (see Table IV; here the H-H and cl-cl results use the same number of gauge field configurations on each set). This reflects slightly lower statistical errors on the 3-point correlators for the H-H current but coupled with a fit function that has also to account for oscillating states.

Set	Action comb'n	$am_s^{\mathrm{H,val}}$	aM_{η_s}	aM_ϕ	af_ϕ/Z_V
1	H-H	0.0705	0.54024(15)	0.8183(33)	0.1994(33)
2	H-H	0.0678	0.52652(4)	0.7966(10)	0.1945(8)
3	H-H	0.0541	0.43134(4)	0.6475(31)	0.1514(38)
5	H-H	0.0533	0.42636(6)	0.6385(18)	0.1510(23)
7	H-H	0.0527	0.42307(2)	0.6336(9)	0.1507(9)
8	H-H	0.0376	0.31389(7)	0.4735(13)	0.1126(12)
9	H-H	0.0360	0.30484(1)	0.4564(6)	0.1082(6)

TABLE VII: Results for the mass of the η_s meson and mass and (unnormalised) decay constants of the ϕ meson in lattice units for the full set of gluon field configurations given in Table I (results for the variable volume sets 4 and 6 will be given in Table VIII). Results for sets 1, 3 and 8 were already given in Tables III and VI. These results are all for correlators made of s quark propagators generated using the HISQ action only. The mass in lattice units of the valence s quarks used in given in column 2.

Set	Action comb'n	L_s/a	$am_s^{\mathrm{H,val}}$	aM_{η_s}	af_{η_s}
4	H-H	24	0.0533	0.42664(9)	0.11257(7)
5	H-H	32	0.0533	0.42636(6)	0.11243(5)
6	H-H	40	0.0533	0.42642(4)	0.11251(3)
5	H-H	32	0.0507	0.41580(10)	0.11122(8)
				aM_ϕ	af_ϕ/Z_V
4	H-H	24	0.0533	0.6390(26)	0.1504(32)
5	H-H	32	0.0533	0.6385(18)	0.1510(23)
6	H-H	40	0.0533	0.6408(14)	0.1526(18)
5	H-H	32	0.0507	0.6337(17)	0.1528(17)

TABLE VIII: Results for the mass and decay constant of the η_s meson (upper table) and the mass and (unnormalised) decay constants of the ϕ meson (lower table) in lattice units for the sets of gluon field configurations of fixed β and sea quark mass parameters but different spatial volume listed in Table I. These results are all for correlators made of s quark propagators generated using the HISQ action only. The mass in lattice units of the valence s quarks used is given in column 4. The results for $am_s^{\mathrm{H,val}}$ of 0.0533 used 1000 configurations from each ensemble (with 16 time sources); those for the deliberately mistuned value (to test tuning uncertainties) of $am_s^{\mathrm{H,val}}$ of 0.0507 used 300 (also with 16 time sources).

Clover propagators are substantially more expensive to calculate since the Dirac matrix is an additional factor of 4 larger in each dimension; clover propagators are also 16 times bigger to store. We see that the extra work associated with the spin degree of freedom does not lead to a reduction in statistical errors for the quantities that we have calculated here. This outcome would clearly be expected for naive quarks because the spin degree of freedom is then completely redundant.

IV. ϕ MESON MASS AND DECAY CONSTANT

The fast inversion of the Dirac matrix for the HISQ action means that we are able to generate propagators and, consequently vector meson correlators, for the full set of gluon field configurations listed in Table I in this case. By fitting the correlators, as described in Section III, we are able to determine the ϕ mass in lattice units and its decay constant using eq. (15). We take results from 6-exponential fits using a $t_{\rm min}$ value of 3 or 4, as for the η_s fits. Results are given in Table VII. This enables us to map out the behaviour of the ϕ mass and decay constant from values of $m_{u/d}$ in the sea of $m_s/5$ all the way down to their physical values and test the results against experiment, and this is what we will do here. First we discuss two systematic effects in the properties of the ϕ meson that we are neglecting in this calculation, and the impact that we expect from this in our results, to be included in our error budget.

The first issue is that we have not included quark-line disconnected diagrams that would allow the $s\overline{s}$ vector to mix with the light isoscalar vector. Phenomenologically this is expected to be a very small effect, as can be seen from the 0.13% branching fraction for the ϕ to decay to $\pi^0\gamma$ [46]. This would be zero for a pure $s\overline{s}$ ϕ and can be compared to the branching fraction of 8% for the isospin zero light vector meson with which it can mix through disconnected diagrams, the ω. There is also evidence for very small effects from lattice QCD calculations that have included quark-line disconnected diagrams. [47] found a mixing angle for $l\bar{l}$ in the ϕ of $1.7(2)^\circ$ at one value of the lattice spacing and a relatively heavy light quark mass. Analysis of quark-line disconnected correlators for the s quark [49], albeit at much heavier sea light quark masses than we use here, can be used to give a systematic error from these missing effects and we will do that below.

Another possible issue to worry about is the fact that the ϕ meson in the real world decays strongly to $K\overline{K}$ and hence is not strictly 'gold-plated'. The ϕ meson mass is close to the threshold for this dominant decay, however, and so the ϕ width is rather small at 4 MeV [46]. A simple model suggests that coupling to the $K\overline{K}$ might contribute -5 MeV to the ϕ mass [18] in the continuum. We expect lattice QCD calculations to be able to reproduce the ϕ meson mass to this level of accuracy then, even if the coupling to the $K\overline{K}$ decay mode is distorted on the lattice.

In lattice QCD calculations the ϕ is stable for two reasons. The first is that the K meson mass depends on the u/d quark mass and so is heavier than its physical value when the u/d are unphysically heavy. We can explore this issue here because we have results for a wide range of u/d quark masses. Note that, in the absence of coupling to $K\overline{K}$, we would expect very little u/d quark mass-dependence for the properties of the ϕ, comparable with that seen for the η_s decay constant (for fixed η_s mass) and mapped out in [22]. The second reason for ϕ stability is that the $\phi \to K\overline{K}$ decay proceeds via a P-wave because the ϕ has spin 1; a zero momentum ϕ must decay to 2 K mesons of equal and opposite non-zero momentum. In the continuum the non-zero momentum can be arbitrarily small, but the minimum lattice spatial momentum is $2\pi/L_s$. The experimental ϕ and K meson masses would require a lattice spatial extent of $L_s \approx 10$ fm for the energy of the decay products to fall below the ϕ mass. This is almost double the size of the largest lattice that we use, typical of state-of-the-art lattice QCD calculations. So in practice this means that ϕ mesons are always stable on the lattice.

We have tested the dependence of the ϕ meson mass and decay constant on the lattice volume for one set of simulation parameters, that corresponding to gluon configuration sets 4, 5 and 6 given in Table I. These sets have the same lattice spacing, $a \approx 0.12$ fm, and $m_{u/d}^{\rm sea} = m_s^{\rm sea}/10$. Their lattice volumes differ from 24 points on a side ($L_s \approx 3$ fm) to 40 points on a side ($L_s \approx 5$ fm). The ϕ mass and decay constant, and those of the η_s, are given in Table VIII. We see that, within the $0.2-0.4\%$ statistical uncertainties that we have, there is no significant effect of the lattice size on the ϕ mass. This is also true for the decay constant within the larger $1-2\%$ uncertainties that we have in that case. A further test comes from the fact that we can fit the independent results on the 3 ensembles simultaneously demanding that they give the same fit parameters for energies and amplitudes and obtain a good fit.

Although we have not calculated the K mass here, we can estimate its value accurately from results at similar masses in [22]. This gives a (Goldstone) K mass in lattice units of 0.315 for the valence s quark mass used here and a u/d quark mass given by that in the sea, so that $2M_K < M_\phi$. However, the value of twice the energy of a K meson with the minimum lattice momentum would vary, in lattice units, from 0.820 on the 24^3 lattice (set 4) to 0.704 on the 40^3 lattice (set 6). The values of $2E_K^{\rm min}$ on all of the volumes are then more than 100 MeV above the corresponding mass of the ϕ. In fact, for staggered quarks, $2E_K^{\rm min}$ would be somewhat higher than these estimates because the ϕ that we use here cannot decay to 2 Goldstone-taste K mesons. Instead we must sum over different appropriate pairs of tastes [38], all of which have masses that are heavier than the Goldstone by an $\mathcal{O}(a^2)$ effect. This then increases further, typically by 50 MeV on these coarse lattices, the discrepancy between M_ϕ and $2E_K$. The finite-volume impact of coupling between ϕ and $K\overline{K}$ is then not visible with our statistical accuracy, because $2E_K$ is too far above M_ϕ.

The only significant finite volume effect that we see in Table VIII is that in the mass of the η_s on the smallest, 24^3, lattices (set 4). At 0.06% the effect is tiny but somewhat larger than the $\mathcal{O}(0.01\%)$ that might have been expected from NLO chiral perturbation theory [22]. A similar effect is seen in aM_π in [48]. Note however that no significant difference is seen between results on the 32^3 and 40^3 lattices. These lattices have sizes in units of M_π of $M_\pi L_s > 4$, more typical of the other ensembles

Error	M_ϕ	f_ϕ
statistics	2.9	2.0
Z_V	-	1.2
$a^2 \to 0$	2.1	1.7
$m_{u/d}$ tuning	0.1	0.1
m_s tuning	0.4	0.4
M_{η_s} value	2.2	-
$K\overline{K}$ decay	2.5	0.7
'disconnected' diagrams	4.0	0.6
Total	6.3	3.1

TABLE IX: Error budget for our results for the mass and decay constant of the ϕ meson. Contributions to the error are given in MeV. The uncertainty from the value of M_{η_s} feeds into M_ϕ (only) since the fitted quantity used to derive M_ϕ is the mass difference. The m_s tuning uncertainty comes from the fit, using a deliberately mistuned s quark mass to assess the impact of the accuracy of our tuning on the quantity being fitted.

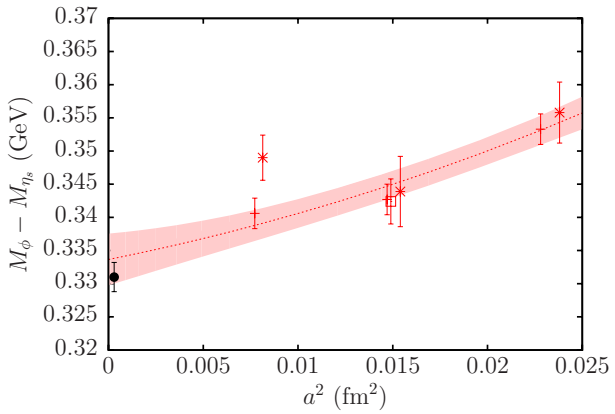

FIG. 9: Results from Table VII for $M_\phi - M_{\eta_s}$ calculated with the HISQ action on a wide range of gluon field configurations and plotted against the square of the lattice spacing. Red bursts give results for u/d quark masses equal to $m_s/5$ (sets 1, 3 and 8), red open squares for $m_{u/d} = m_s/10$ (set 5), and red pluses for $m_{u/d}$ close to its physical value (sets 2, 7 and 9). Note that the result for a mistuned s mass, included in the fit, is not plotted. Error bars include statistical errors and uncertainties from the lattice spacing that are correlated between the points. The red shaded band and dotted red line give the result of a chiral/continuum fit described in the text, evaluated at physical $m_{u/d}$ as a function of lattice spacing. The black filled circle gives the value corresponding to the difference of the experimental ϕ meson mass the mass of the η_s determined from lattice QCD [22]. It is offset slightly from $a = 0$ for visibility.

used here.

We now move on to look at how the ϕ meson mass is affected by the u/d quark mass in the sea. Our results, in Table VII, include u/d quark masses from $m_s/5$ down to the physical value ($m_s/27.4$ [46]). The spatial size of the lattices, L_s, is approximately constant in units of M_π with $M_\pi L_s$ values varying from 3.3 to 4.6 [22]. The minimum energy of virtual $K\overline{K}$ pairs then falls linearly with $m_{u/d}$ towards the physical point both as M_K falls and as the minimum spatial momentum falls. We might then expect to see some impact on M_ϕ from changing $m_{u/d}$. As an example, on the fine physical point lattices (set 9) the minimum $2E_K$ for the Goldstone K meson is only 40 MeV above M_ϕ. Staggered taste-effects, reduced by over a factor of two compared to the coarse lattices discussed above, typically gives a further 20 MeV. The impact of taste-effects means that we need to allow for a^2-dependent $m_{u/d}$ effects in our fits used to determine the physical (continuum and chiral) limit of our results, and we will do this below.

Figure 9 shows our results for the difference of the ϕ and η_s masses as a function of lattice spacing. We use the difference, as we did in Section III F, rather than the ϕ mass itself, to reduce uncertainties from the lattice spacing[4]. The different symbols indicate results at different values of the u/d quark mass. We see that on the fine lattices there seems to be a difference between results at $m_{u/d}/m_s = 1/5$ (red burst) and $m_{u/d}$ at its physical value (red plus), whereas there is no clear difference on the very coarse lattices. This is consistent with the expectation above, but is not very significant given our statistical uncertainties.

To extract a physical result we fit the results to a simple functional form in a^2 and $m_{u/d}$, allowing for correlations between the points coming from the determination of the lattice spacing. The functional form that we use is:

$$\begin{aligned}[M_\phi - M_{\eta_s}](a, m_{u/d}) = [M_\phi - M_{\eta_s}]_{\rm phys} \times \\ \left[1 + c_{a^2}(\Lambda a)^2 + c_{a^4}(\Lambda a)^4 + c_{a^6}(\Lambda a)^6\right. \\ + c_\delta \frac{\delta m}{10}(1 + c_{\delta a^2}(\Lambda a)^2) \\ \left. + c_s(M_{\eta_s} - 0.6885\,{\rm GeV})\right]. \end{aligned} \quad (16)$$

Here $[M_\phi - M_{\eta_s}]_{\rm phys}$ is the physical value in the continuum and chiral limit; we take a prior of 0.3(1) on this value. Coefficients c_{a^n} allow for discretisation effects; we take priors of 0.0(1.0) on these values, except for c_{a^2} for which we take 0.0(0.5) since there are no tree-level a^2 errors in the HISQ action [8]. In fact the higher order terms, c_{a^4} and c_{a^6}, have little impact on the fit. c_δ allows for the effect of unphysical u/d quark masses and $c_{\delta a^2}$ for a^2-dependence in these effects. Here δm is difference of $2m^{\rm sea}_{u/d} + m^{\rm sea}_s$ and its tuned value in units of the tuned s quark mass [24]. Dividing by 10 converts it into a chiral scale. We take very wide priors of 0.0(5.0) on c_δ and $c_{\delta a^2}$ to allow for the effects of $K\overline{K}$ coupling to the ϕ giving more pronounced dependence than is normally seen in gold-plated meson masses. In fact the width of this prior makes little difference to the physical point result. Fi-

[4] A fit to the ratio M_ϕ/M_{η_s} also avoids large lattice spacing uncertainties but the statistical errors in the ϕ mass lead to a larger uncertainty in M_ϕ at the physical point.

nally, c_s allows for slight mistunings of the s quark mass, as measured by mistuning of M_{η_s}. Here we make use of the results given in Table VIII at a deliberately mistuned valence s mass of 0.0507 to estimate this parameter and include these results to enable it to be fixed within the fit. We take the prior on c_s of -0.5(0.5).

The fit gives a χ^2/dof of 0.97 for 8 degrees of freedom (the 7 tuned s mass data points plus the mistuned value). The fitted curve evaluated at the physical sea quark masses ($\delta m = 0.0$) is plotted as a red band in Figure 9. The physical result is 0.335(4) GeV in good agreement with the value expected from the experimental ϕ mass of 0.331(2) GeV. This is a significant improvement on our earlier value [18] using gluon field configurations that include 2+1 flavours of asqtad quarks in the sea but at heavier-than-physical u/d quark masses. Adding back in the η_s meson mass, with its 2.2 MeV uncertainty, gives a lattice QCD result of

$$M_\phi = 1.0232(42)(25)(40)\,\text{GeV} \qquad (17)$$

to compare to the experimental result of 1.0195 GeV [46] (with a sub-MeV uncertainty). Here the second error of 2.5 MeV is included to allow for the incomplete treatment of the $K\overline{K}$ decay mode. We take this as half the expected shift in M_ϕ from coupling to $K\overline{K}$, given that there is evidence in our results of sea u/d quark mass-dependence consistent with some impact from this effect. The third error, of 4 MeV, allows for the missing quark-line disconnected correlators. In [49], the same result for the ϕ mass was found, to an accuracy of 0.4%, whether quark-line disconnected diagrams were included in the fit or not, so we take this as the uncertainty. Our error budget is given in Table IX.

Our analysis of the ϕ meson decay constant proceeds in a similar way to that of the mass. Figure 10 plots the results from Table VII as a function of lattice spacing. To convert the results for af_ϕ/Z_V in Table 10, obtained directly from the ground-state amplitudes of fits to our 2-point correlators, into results in physical units for f_ϕ we need to multiply by a^{-1} in GeV from Table I and the current renormalisation, Z_V from Table IV. We have determined Z_V on only one ensemble from each group with almost the same lattice spacing. However, we do not expect Z_V to vary significantly between for example, sets 3, 5 and 7. Physically Z_V relates currents between two different regularisations of QCD (the continuum and the lattice) that differ in their ultraviolet modes. It can be expressed in QCD perturbation theory (although we have chosen to calculate it nonperturbatively) as a power series in α_s where the scale of α_s is related to the inverse lattice spacing. The Z_V values we have for the HISQ case are very close to 1, with a difference of 1 of about 0.01. Assuming this comes purely from an $\mathcal{O}(\alpha_s)$ term we can estimate the effect on Z_V of the small changes in a between sets 3 and 7 of 2%. This gives an expected change in Z_V of 0.0001, smaller than our uncertainties. We therefore use the Z_V results from Table IV to renormalise the results from all of our ensembles, including the uncertainty from Z_V, and its correlation between sets of results, in our continuum/chiral fit.

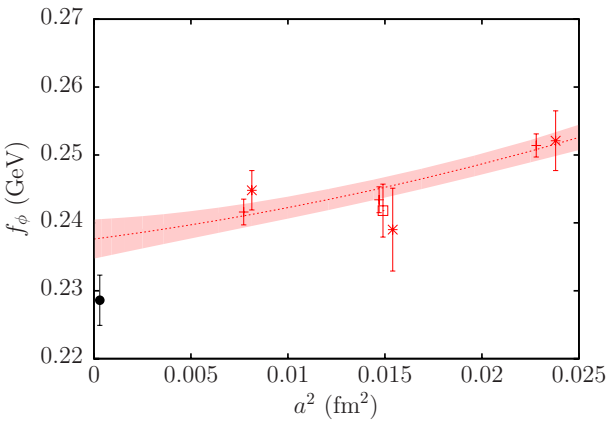

FIG. 10: Results from Table VII for f_ϕ, the ϕ meson decay constant, calculated with the HISQ action on a wide range of gluon field configurations and plotted against the square of the lattice spacing. Red bursts give results for u/d quark masses equal to $m_s/5$ (sets 1, 3 and 8), red open squares for $m_{u/d} = m_s/10$ (set 5), and red pluses for $m_{u/d}$ close to its physical value (sets 2, 7 and 9). Note that the result for a mistuned s mass, included in the fit, is not plotted. Error bars include statistical errors and uncertainties from the lattice spacing and current renormalisation factor Z_V that are correlated between the points. The red shaded band and dotted red line give the result of a chiral/continuum fit described in the text, evaluated at physical $m_{u/d}$ as a function of lattice spacing. The black filled circle gives the value inferred from the experimental width for ϕ decay to e^+e^- [46]. It is offset slightly from $a = 0$ for visibility.

Our continuum and chiral fit for f_ϕ takes exactly the same form as that given in Eq. 16 and has the same priors, except for the prior on the physical result which we now take to be 0.2(0.1) and on c_s which we take as 0.0(0.5) as there is no phenomenological reason to expect a strong dependence in either direction for the effect of mistuning the s quark mass. Our fitted curve evaluated at physical sea quark masses is shown as the shaded band on Figure 10. The physical result that we obtain (with a χ^2/dof of 0.71 for 8 degrees of freedom) is

$$f_\phi = 0.2376(29)(7)(6)\,\text{GeV}. \qquad (18)$$

This is in reasonable agreement (within 2σ) of the result of 0.2285(36) GeV inferred from experiment (see eq. (14)) and again is a signficant improvement on our earlier result [18]. The second uncertainty here is an estimate of the impact of coupling to the $K\overline{K}$ decay mode. We take an estimate of 20 MeV for the difference of ρ and ω decay constants inferred from their leptonic decay rates and multiply by the ratio of ϕ to ρ total widths [46] (4/150) and the ratio of ϕ to ω decay constants (0.23/0.2). The ρ decays strongly to $\pi\pi$ but the ω, having isospin zero, cannot do this. The large width of the ρ makes the determination of its decay constant problematic but a 20 MeV

difference between ρ and ω results from the application of eq. (14) [49], remembering to allow for the isospin difference between the two mesons that reduces the 'effective charge' in the ω case to one third that of the ρ. If we assume that the 20 MeV is an indication of the size of effects from strong decays then reducing this in proportion to the total width of ρ and ϕ and increasing in proportion to the decay constant gives an estimate of 0.6 MeV for the impact on the ϕ. The third uncertainty, of 0.7 MeV, is an estimate of the impact of missing quark-line disconnected diagrams. We obtain this from the analysis in [49], where the effect of the disconnected $s\bar{s}$ correlator on the anomalous magnetic moment of the muon was found to be -0.05% of that of the light-quark connected correlator. This is equivalent to -0.5% of the s-quark connected correlator (for the light quark masses used there). Taking the connected correlator contribution to be approximately proportional to the square of the decay constant [49] implies a -0.3% effect on the decay constant. Rather than take this as a one-sided error, we simply take the value as an estimate of the uncertainty.

V. CONCLUSIONS

The results presented here range over an apparently rather broad set of topics but they are all linked through the necessity to reduce and to test uncertainties obtained from lattice QCD calculations for decay rates that can be compared to experiment. We have focussed here on mesons made from valence s quarks because, although the s quark is light in QCD terms s quark propagators are considerably faster to generate in lattice QCD than those containing u/d quarks and correlators are statistically more precise, enabling systematic effects to be more clearly seen. We work on state-of-the-art gluon field configurations that include the effect of u, d, s and c quarks in the sea with an improved gluon action to minimise systematic discretisation effects coming from anywhere other than the different quark actions that we compare.

Our first analysis here has compared renormalisation constants, determined nonperturbatively, for temporal axial vector and temporal vector currents constructed either from HISQ quarks or from clover quarks or, in a mixed-action approach, from one clover and one HISQ quark. For the temporal axial current case we have used the fact that pseudoscalar correlators made from HISQ quarks can be absolutely normalised. For the temporal vector case we have used the fact that the vector form factor between two identical mesons at rest should be 1. Our results show that the renormalisation constants for the clover-clover case are very different from 1, as expected from one-loop perturbation theory, but that the mixed-action currents inherit elements of this renormalisation in a relatively simple way, as suggested by the work of [12]. This means that the ratio of the mixed action renormalisation constant to the square root of the product of the renormalisation constants for the local temporal vector currents for the unmixed action cases (i.e. ρ in eq. (3)) is close to 1. Our nonperturbative test of this relationship means that it is indeed valid to calculate this ratio to one-loop in lattice QCD perturbation theory and take a small uncertainty (of $\mathcal{O}(1\%)$) from missing higher order terms, as the Fermilab Lattice/MILC collaborations do in their work on B and D meson decay constants [15] and $B \to \pi\ell\nu$ form factors [16] using a mixed clover-staggered approach. Thus our results provide confirmation, after the fact, of this element of their error budget. In Appendix A we show a similar perturbative analysis for mixed NRQCD-light currents, justifying the normalisation element of the error budget in the B decay constant [14] and $B \to \pi\ell\nu$ calculations [50] in this case.

Modifications to the Fermilab heavy quark approach have been used in the Relativistic Heavy Quark (RHQ) formalism [51] by the RBC/UKQCD collaboration [52, 53]. The modifications involve tuning some coefficients nonperturbatively to reduce leading systematic errors. The approach to the normalisation of heavy-light currents is the same, however, using eq. (1) to define the ratio ρ and then determining ρ to one-loop in lattice QCD perturbation theory. The coefficient of α_s in ρ is somewhat larger for the RHQ-domain wall current than in the Fermilab-asqtad case, but it is still numerically small at 0.1 [52] for the temporal axial current. The uncertainty in f_B and $B \to \pi$ form factors from missing higher-order terms in the perturbative expansion is taken as the size of the one-loop term in ρ, arguing that, as for the Fermilab case, the one-loop term is indicative of what will appear at higher orders. Our results are not directly applicable to this case and it is harder to argue about the 'natural' size of perturbative coefficients when there are relatively large nonperturbative coefficients (such as that of the clover term) in the action. It would be straightforward to provide a consistency check by repeating the analysis that we have done here, substituting a light RHQ field for the clover quark and a domain-wall quark for the HISQ quark.

Such tests are important because lattice QCD determination of these decay constants and form factors feeds into determination of CKM elements such as V_{ub} through comparison with experimental exclusive decay modes. Accuracy on CKM elements is critical to overconstraining the Standard Model in the search for new physics. Currently the discrepancy in V_{ub} determination using inclusive and exclusive processes is a cause for concern [46] and resolution will require improved accuracy from both determinations. On the exclusive side, we need to be sure that we understand sources of uncertainty in the lattice QCD calculation and our result here provides reassurance that we do understand uncertainties from current normalisation.

Our further analysis has focussed on the mass and decay constant of ϕ mesons, using the vector current renormalisation factors to fix the normalisation of the decay constant. We have seen that the results from all three possibilities, using the HISQ action or the clover action

or the mixed-action approach, agree in the continuum limit as they should on a set of ensembles with a fixed heavier-than-physical u/d quark mass. This is an important and independent consistency check of our results and they show, as expected, larger discretisation effects with the clover action than with the more highly improved HISQ action.

To study the mass and decay constant of the ϕ meson closer to the physical point, we have used the HISQ action (only) on a wider set of gluon field configurations that include different values of the u/d quark masses in the sea going down to the physical value. We include single-meson quark-line connected diagrams only since we believe, based on phenomenological evidence, that the impact of quark-line disconnected diagrams and coupling of the ϕ to its $K\overline{K}$ decay mode, which is virtual on the lattice, is small. We may be seeing some evidence of the effect of this coupling in enhanced dependence of the ϕ meson mass on the u/d sea quark mass. Our final results are:

$$\begin{aligned} M_\phi &= 1.0232(42)(25)(40)\,\text{GeV} \\ f_\phi &= 0.2376(29)(7)(6)\,\text{GeV}. \end{aligned} \tag{19}$$

The second error in both cases is an estimate of the remaining effect of the $K\overline{K}$ mode, and the third error, an estimate of the impact of missing quark-line disconnected diagrams. Our results are in good agreement with experiment and the $\mathcal{O}(5\,\text{MeV})$ uncertainties are a significant improvement on earlier results. The accuracy of our ϕ meson correlators led to the first flavour-separated determination of the valence s quark hadronic vacuum polarisation contribution to the anomalous magnetic moment of the muon [28]; an uncertainty of 1% was reached in that calculation. These uncertainties are also promising for improvements to lattice QCD calculations of form factors for decay processes that include ϕ mesons [18, 20].

Acknowledgements

We are grateful to the MILC collaboration for the use of their configurations and to R. Dowdall, A. El-Khadra, E. Gámiz, A. Kronfeld and R. van de Water for useful discussions. Computing was done on the Darwin supercomputer at the University of Cambridge as part of STFC's DiRAC facility. We are grateful to the Darwin support staff for assistance. Funding for this work came from the Gilmour bequest to the University of Glasgow, the National Science Foundation, the Royal Society, the Science and Technology Facilities Council and the Wolfson Foundation. B. C. is supported by the U.S. Department of Energy Office of Science, Office of Nuclear Physics under contract DE-AC05-06OR23177.

NRQCD-clover			
Ma	n	$z_0^{(1)}$	$\rho^{(1)}$
4.0	2	-0.2972	-0.0077
3.0	2	-0.3533	-0.0638
2.0	2	-0.3002	-0.0107
1.2	3	-0.2096	+0.0799
NRQCD-asqtad			
Ma	n	$z_0^{(1)}$	$\rho^{(1)}$
4.0	2	0.272	0.067
2.8	2	0.209	0.0035
1.95	4	0.154	-0.052
1.2	6	0.154	-0.052
NRQCD-HISQ			
Ma	n	$z_0^{(1)}$	$\rho^{(1)}$
3.297	4	0.024	0.082
2.66	4	0.006	0.064
1.91	4	-0.007	0.051

TABLE X: Results for one-loop coefficients for the renormalisation of the lattice NRQCD-light temporal axial current for (from top to bottom) clover, asqtad and HISQ light quarks. Columns 1 and 2 given the bare lattice NRQCD mass and the stability parameter, n [31]. For the NRQCD-clover results, $z_0^{(1)}$ is taken from [9] where it is called ρ_0. For NRQCD-asqtad $z_0^{(1)}$ is obtained as $\tilde{\rho}_0 - \zeta_{10}$ from [10]. For NRQCD-HISQ $z_0^{(1)}$ is taken from [14]. Values of $\rho^{(1)}$ make use of the appropriate $z_l^{(1)}$ as given in the text.

Appendix A: Renormalisation of NRQCD-light currents

An interesting question is whether this approach, in which the renormalisation constant for a mixed-action operator is defined in terms of renormalisation constants for the temporal vector current for the associated single-action operators, also works for other actions in terms of giving a perturbative series for the remainder which is closer to 1. Here we test this for the case of the heavy-light temporal axial current operator that combines an NRQCD [5] heavy quark with a light clover, asqtad or HISQ quark.

Through order $\mathcal{O}(\Lambda/M)$ in an inverse heavy quark mass expansion, we define the renormalisation constant for the lattice NRQCD-light operator by [14]

$$A^4_{\text{cont QCD}} = Z_{A^4,\text{NRQCD}}(J^{(0)} + J^{(1)}). \tag{A1}$$

Here $J^{(0)}$ and $J^{(1)}$ are the leading and next-to-leading order operators in the Λ/M expansion whose matrix elements between the vacuum and a B-meson are readily calculated in lattice QCD [14]. $Z_{A^4,\text{NRQCD}}$ has been calculated through $\mathcal{O}(\alpha_s)$ for the combination of NRQCD heavy quarks with clover light quarks [9], asqtad light quarks [10] and HISQ light quarks [11, 14] (in all cases setting the light quark mass to zero). Writing

$$Z_{A^4,\text{NRQCD}-\text{light}} = 1 + z_0^{(1)}\alpha_s + \ldots \tag{A2}$$

gives the values for z_0 given in Table X for a selection of NRQCD bare quark masses in lattice units.

A test of the renormalisation method advocated by the Fermilab collaboration is then to compare the perturbative series for ρ_{A^4} where

$$\rho^{A^4,\mathrm{NRQCD-light}} = \frac{Z_{A^4,\mathrm{NRQCD-light}}}{\sqrt{Z_{V^4,\mathrm{NRQCD-NRQCD}} Z_{V^4,\mathrm{light-light}}}}, \tag{A3}$$

as the analogue of Eq. (1). Here we take for $Z_{V^4,\mathrm{NRQCD-NRQCD}}$ the renormalisation factor for the NRQCD-NRQCD temporal current in scattering, and this is 1 for equal masses [54]. The light-light renormalisation factor for massless quarks can be written as

$$Z_{V^4,\mathrm{light-light}} = 1 + z_l^{(1)}\alpha_s + \ldots \tag{A4}$$

and then, if

$$\rho^{A^4,\mathrm{NRQCD-light}} = 1 + \rho^{(1)}\alpha_s + \ldots \tag{A5}$$

then $\rho^{(1)} = z_0^{(1)} - z_l^{(1)}/2$. The success of the method can then be judged by comparing the smallness of $\rho^{(1)}$ with that of $z_0^{(1)}$.

Table X gives values for $\rho^{(1)}$ for a variety of light-quark actions. For the tadpole-improved clover action, with a clover coefficient $c_{sw} = 1$, on a gluon field from a simple plaquette action, which is appropriate to the z_0 calculation given in [9], we use [41, 42]

$$z_l^{(1)} = -1.6261 - u_0^{(1)} \tag{A6}$$

where $u_0^{(1)}$ is the one-loop coefficient of the tadpole parameter u_0 by which the gluon fields are divided. This division removes large and universal tadpole effects [30]. If the value of u_0 is taken as the fourth root of the average plaquette, then $u_0^{(1)} = -\pi/3$. This gives $z_l^{(1)} = -0.579$. For asqtad quarks, again using tadpole-improvement with u_0 set by the mean plaquette as appropriate to the z_0 values, and a Symanzik-improved gauge action, $z_l^{(1)} = 0.411$ [55]. For HISQ quarks on Symanzik-improved gluon fields, $z_l^{(1)} = -0.1164(3)$ (Section B).

We see from Table X that the perturbative expansion of ρ looks much better than that of z_0, as judged by the one-loop coefficients, for the NRQCD-clover and NRQCD-asqtad results. The effect of using eq. (A3) is to remove a constant factor coming from the light quark action in those cases (nothing is required for the NRQCD action). The remaining coefficients are generally then of approximately the same magnitude as the value quoted in Section III D for the massless clover-asqtad case, i.e. around 0.05.

For the NRQCD-HISQ case, the coefficient $\rho^{(1)}$ is actually larger in magnitude than $z_0^{(1)}$ and so, although $\rho^{(1)}$ is not large, it makes no sense to apply eq. (A3). The HISQ action needs so little renormalisation that correcting for a renormalisation issue that is not there is counterproductive. This is why in the current state-of-the-art determination using NRQCD of the B and B_s meson decay constants [14] and corresponding vector meson results [56] we simply applied the formula of eq. (A2) (along with additional current corrections that appear at $\alpha_s\Lambda/m_b$).

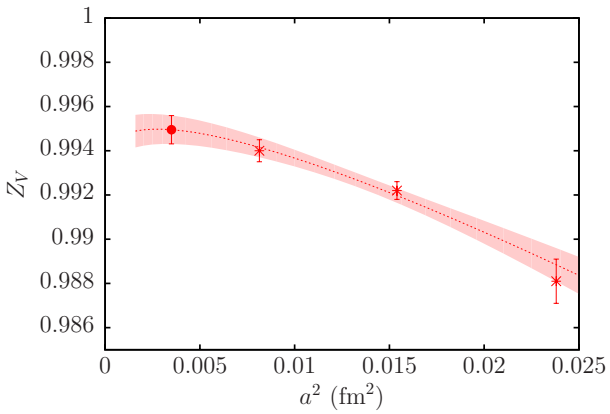

FIG. 11: The renormalisation factor, Z_V, for the local temporal vector current between HISQ quark fields, plotted against the square of the lattice spacing. Results from Table IV are plotted as red bursts; the red band gives the fit to a perturbative expansion with discretisation effects described in the text. The red filled circle gives the extrapolated result on superfine lattices with $a = 0.059$ fm.

Appendix B: Z factors for the Future

Given that the Z factors for the vector current can be determined very precisely by the nonperturbative method discussed in Section III C it is worth asking: a) how well can they be matched to perturbative expectations? and b) how well can we extrapolate the results to finer lattices? The reason for asking question b) is that the determination of Z_V for the local HISQ temporal vector current using a 3-point function with clover spectator quark is numerically expensive. A numerically faster method is to use the RI-SMOM scheme [57], being adapted for the HISQ action [58], but here we investigate extrapolation as a way to remove the need for additional calculations. Since Z_V, as a perturbative expansion in α_s, changes only slowly with lattice spacing it should be possible to extrapolate results to finer lattices without large uncertainties. Such an extrapolation, however, must include terms to allow for nonperturbative discretisation effects that will be present.

To test this we fit the H-H Z_V results from Table IV to the following form:

$$Z_V(a,\alpha_s) = \sum_{i=0}^{n_i}\left[c_i + d_i(\frac{a\Lambda}{\pi})^2 + f_i(\frac{a\Lambda}{\pi})^4\right]\alpha_s^i \tag{B1}$$

where α_s is taken in the $\overline{\mathrm{MS}}$ scheme at a scale of $2/a$, although using $1/a$ or $3/a$ makes little difference. c_0 is taken as 1.0 and c_1 = -0.1164(3) from lattice QCD perturbation theory [59]. The other c_i, and the d_i and f_i, are given priors of 0.0(1.0). We take $\Lambda = 0.5$ GeV and

a discretisation effect dependent on $a\Lambda/\pi$ suitable for an ultraviolet quantity such as Z, since the momentum cutoff on the lattice is π/a. Using $n_i = 5$ gives the fit curve plotted in Figure 11; increasing n_i beyond this makes no difference, and decreasing n_i to 3 also has little impact. The fit has a χ^2/dof of 0.8 and favours a positive and fairly sizeable (although quite uncertain) coefficient at α_s^2 of 0.59(16).

This enables us to predict the value of Z_V on superfine lattices (with $a = 0.059$fm) with an accuracy of 0.06% as 0.9950(6). The dominant uncertainty (0.06%) comes from the statistical uncertainties on the Z factors on coarser lattices, with 0.01% coming from the a^2 extrapolation and 0.02% from the perturbative series. We have checked that the extrapolated superfine result is not affected significantly (less than 1σ) by missing out the value on the coarsest lattices from the fit. A further check of the result and its uncertainty comes from fitting the results on the coarsest two lattices to predict a value for the fine lattice. This gives 0.9948(10), in good agreement (within 1σ) of the actual value we have calculated there of 0.9940(5) (see Table IV). Using our fit to the full set of results we can also obtain a value for Z_V for ultrafine lattices (with $a = 0.044$ fm) of 0.9949(7).

These uncertainties are small enough to mean that the Z factors will not cause a dominant uncertainty in the calculation, for example, of the hadronic vacuum polarisation contribution to the anomalous magnetic moment of the muon on these finer lattices [38]. Note that these results are for a current composed of s quarks. We have not studied the dependence on quark mass of the Z factors; from perturbation theory it should be small, with a leading term of $\alpha_s(ma)^2$.

[1] C. Davies, PoS **LATTICE2011**, 019 (2011), 1203.3862.
[2] J. Laiho, E. Lunghi, and R. Van de Water, PoS **LATTICE2011**, 018 (2011), 1204.0791.
[3] C. McNeile, C. Davies, E. Follana, K. Hornbostel, and G. Lepage, Phys.Rev. **D82**, 034512 (2010), 1004.4285.
[4] C. McNeile, C. Davies, E. Follana, K. Hornbostel, and G. Lepage, Phys.Rev. **D85**, 031503 (2012), 1110.4510.
[5] G. P. Lepage, L. Magnea, C. Nakhleh, U. Magnea, and K. Hornbostel, Phys.Rev. **D46**, 4052 (1992), hep-lat/9205007.
[6] A. X. El-Khadra, A. S. Kronfeld, and P. B. Mackenzie, Phys.Rev. **D55**, 3933 (1997), hep-lat/9604004.
[7] E. Follana, C. Davies, G. Lepage, and J. Shigemitsu (HPQCD Collaboration, UKQCD Collaboration), Phys.Rev.Lett. **100**, 062002 (2008), 0706.1726.
[8] E. Follana et al. (HPQCD Collaboration, UKQCD Collaboration), Phys.Rev. **D75**, 054502 (2007), hep-lat/0610092.
[9] C. J. Morningstar and J. Shigemitsu, Phys.Rev. **D59**, 094504 (1999), hep-lat/9810047.
[10] E. Dalgic, J. Shigemitsu, and M. Wingate, Phys.Rev. **D69**, 074501 (2004), hep-lat/0312017.
[11] C. Monahan, J. Shigemitsu, and R. Horgan, Phys.Rev. **D87**, 034017 (2013), 1211.6966.
[12] J. Harada, S. Hashimoto, K.-I. Ishikawa, A. S. Kronfeld, T. Onogi, et al., Phys.Rev. **D65**, 094513 (2002), hep-lat/0112044.
[13] A. X. El-Khadra, E. Gamiz, A. S. Kronfeld, and M. A. Nobes, PoS **LAT2007**, 242 (2007), 0710.1437.
[14] R. Dowdall, C. Davies, R. Horgan, C. Monahan, and J. Shigemitsu (HPQCD Collaboration), Phys.Rev.Lett. **110**, 222003 (2013), 1302.2644.
[15] A. Bazavov et al. (Fermilab Lattice, MILC), Phys. Rev. **D85**, 114506 (2012), 1112.3051.
[16] J. A. Bailey et al. (Fermilab Lattice, MILC), Phys. Rev. **D92**, 014024 (2015), 1503.07839.
[17] B. Aubert et al. (BaBar Collaboration), Phys.Rev. **D78**, 051101 (2008), 0807.1599.
[18] G. C. Donald, C. T. H. Davies, J. Koponen, and G. P. Lepage (HPQCD), Phys. Rev. **D90**, 074506 (2014), 1311.6669.
[19] J. Hietala, D. Cronin-Hennessy, T. Pedlar, and I. Shipsey, Phys. Rev. **D92**, 012009 (2015), 1505.04205.
[20] R. R. Horgan, Z. Liu, S. Meinel, and M. Wingate, Phys. Rev. Lett. **112**, 212003 (2014), 1310.3887.
[21] C. T. H. Davies, E. Follana, I. D. Kendall, G. P. Lepage, and C. McNeile (HPQCD), Phys. Rev. **D81**, 034506 (2010), 0910.1229.
[22] R. J. Dowdall, C. T. H. Davies, G. P. Lepage, and C. McNeile, Phys. Rev. **D88**, 074504 (2013), 1303.1670.
[23] T. Bakeyev, M. Gockeler, R. Horsley, D. Pleiter, P. E. L. Rakow, G. Schierholz, and H. Stuben (QCDSF-UKQCD), Phys. Lett. **B580**, 197 (2004), hep-lat/0305014.
[24] B. Chakraborty, C. T. H. Davies, B. Galloway, P. Knecht, J. Koponen, G. Donald, R. Dowdall, G. Lepage, and C. McNeile, Phys. Rev. **D91**, 054508 (2015), 1408.4169.
[25] S. Borsanyi et al., JHEP **09**, 010 (2012), 1203.4469.
[26] A. Bazavov et al. (MILC Collaboration), Phys.Rev. **D87**, 054505 (2013), 1212.4768.
[27] A. Hart, G. M. von Hippel, and R. R. Horgan (HPQCD), Phys. Rev. **D79**, 074008 (2009), 0812.0503.
[28] B. Chakraborty, C. T. H. Davies, G. C. Donald, R. J. Dowdall, J. Koponen, G. P. Lepage, and T. Teubner (HPQCD), Phys. Rev. **D89**, 114501 (2014), 1403.1778.
[29] T. DeGrand and C. E. Detar, *Lattice methods for quantum chromodynamics* (2006).
[30] G. P. Lepage and P. B. Mackenzie, Phys. Rev. **D48**, 2250 (1993), hep-lat/9209022.
[31] R. J. Dowdall et al. (HPQCD), Phys. Rev. **D85**, 054509 (2012), 1110.6887.
[32] G. P. Lepage, B. Clark, C. Davies, K. Hornbostel, et al., Nucl. Phys. Proc. Suppl. **106**, 12 (2002), hep-lat/0110175.
[33] M. Wingate, J. Shigemitsu, C. T. H. Davies, G. P. Lepage, and H. D. Trottier, Phys. Rev. **D67**, 054505 (2003), hep-lat/0211014.
[34] E. B. Gregory et al., Phys. Rev. **D83**, 014506 (2011), 1010.3848.
[35] C. T. H. Davies, C. McNeile, E. Follana, G. P. Lepage, H. Na, and J. Shigemitsu, Phys. Rev. **D82**, 114504 (2010), 1008.4018.

[36] A. Bazavov et al. (Fermilab Lattice, MILC), Phys. Rev. **D90**, 074509 (2014), 1407.3772.
[37] G. C. Donald, C. T. H. Davies, R. J. Dowdall, E. Follana, K. Hornbostel, J. Koponen, G. P. Lepage, and C. McNeile, Phys. Rev. **D86**, 094501 (2012), 1208.2855.
[38] B. Chakraborty, C. T. H. Davies, P. G. de Oliviera, J. Koponen, and G. P. Lepage (2016), 1601.03071.
[39] S. R. Sharpe and A. Patel, Nucl. Phys. **B417**, 307 (1994), hep-lat/9310004.
[40] Y. Taniguchi and A. Ukawa, Phys. Rev. **D58**, 114503 (1998), hep-lat/9806015.
[41] M. Luscher, S. Sint, R. Sommer, and H. Wittig, Nucl. Phys. **B491**, 344 (1997), hep-lat/9611015.
[42] S. Capitani, M. Gockeler, R. Horsley, H. Perlt, P. E. L. Rakow, G. Schierholz, and A. Schiller, Nucl. Phys. **B593**, 183 (2001), hep-lat/0007004.
[43] A. Skouroupathis and H. Panagopoulos, Phys. Rev. **D79**, 094508 (2009), 0811.4264.
[44] J. A. Bailey et al. (Fermilab Lattice, MILC), Phys. Rev. **D89**, 114504 (2014), 1403.0635.
[45] J. Harada, S. Hashimoto, A. S. Kronfeld, and T. Onogi, Phys. Rev. **D65**, 094514 (2002), hep-lat/0112045.
[46] C. Patrignani et al. (Particle Data Group), Chin. Phys. **C40**, 100001 (2016).
[47] J. J. Dudek, R. G. Edwards, P. Guo, and C. E. Thomas (Hadron Spectrum), Phys. Rev. **D88**, 094505 (2013), 1309.2608.
[48] A. Bazavov et al. (MILC), Phys. Rev. Lett. **110**, 172003 (2013), 1301.5855.
[49] B. Chakraborty, C. T. H. Davies, J. Koponen, G. P. Lepage, M. J. Peardon, and S. M. Ryan, Phys. Rev. **D93**, 074509 (2016), 1512.03270.
[50] B. Colquhoun, R. J. Dowdall, J. Koponen, C. T. H. Davies, and G. P. Lepage, Phys. Rev. **D93**, 034502 (2016), 1510.07446.
[51] N. H. Christ, M. Li, and H.-W. Lin, Phys. Rev. **D76**, 074505 (2007), hep-lat/0608006.
[52] N. H. Christ, J. M. Flynn, T. Izubuchi, T. Kawanai, C. Lehner, A. Soni, R. S. Van de Water, and O. Witzel, Phys. Rev. **D91**, 054502 (2015), 1404.4670.
[53] J. M. Flynn, T. Izubuchi, T. Kawanai, C. Lehner, A. Soni, R. S. Van de Water, and O. Witzel, Phys. Rev. **D91**, 074510 (2015), 1501.05373.
[54] P. Boyle and C. Davies (UKQCD), Phys. Rev. **D62**, 074507 (2000), hep-lat/0003026.
[55] J. Kim, W. Lee, and S. R. Sharpe, Phys. Rev. **D81**, 114503 (2010), 1004.4039.
[56] B. Colquhoun, C. T. H. Davies, R. J. Dowdall, J. Kettle, J. Koponen, G. P. Lepage, and A. T. Lytle (HPQCD), Phys. Rev. **D91**, 114509 (2015), 1503.05762.
[57] C. Sturm, Y. Aoki, N. H. Christ, T. Izubuchi, C. T. C. Sachrajda, and A. Soni, Phys. Rev. **D80**, 014501 (2009), 0901.2599.
[58] A. T. Lytle (LATTICE-HPQCD), PoS **LATTICE2015**, 258 (2016), 1511.06547.
[59] H. Trottier, private communication (2008).